The Ultimate Compressive Strength of Thin Sheet Metal Panels

Thesis by

E. E. Sechler

In partial Fulfillment of the Requirements for the Degree of

Doctor of Philosophy, California Institute of Technology, Pasadena, California

1934

Contents

Summary

In this report of work on the ultimate strength of thin sheet metal panels, the general formulas for the design of such panels has been developed. Two important equations have been obtained by theoretical reasoning, namely that the total load carried in compression by any unstiffened, simply supported panel can be given by

$$P = C\sqrt{E\sigma}\,t^2$$

and that the constant C is given by

$$C = f(\lambda,\eta) = f\left(\sqrt{\frac{E}{\sigma}}\frac{t}{b},\ \sqrt{\frac{E}{\sigma}}\frac{b}{R}\right)$$

where E = the Young's modulus of the material

σ = the stress at the supported edges

t = the thickness of the material

b = the width of the panel

R = the radius of curvature of the panel

This treatment has then been extended to the case of stiffened panels, both flat and curved, and the predicted loads have been found to give a good check with the loads obtained by actual failure tests of such panels.

Design curves are given to facilitate calculations and complete calculations of particular cases are carried out in the Appendices.

Appreciation

The author wishes to express his appreciation of the assistance furnished by members of the staff of the Guggenheim Graduate School of Aeronautics at the California Institute of Technology and also of the services rendered by members of the graduate and undergraduate student body. In particular he wishes to thank Doctors von Karman, Klein, C. B. Millikan, and Donnell for their helpful suggestions and criticisms. Also Mr. Raymond of the Douglas Aircraft Co., who aided by suggestions making the work more applicable to practical design.

Gratitude is also expressed to the Massachusetts Institute of Technology, and in particular to Professor Newell of that institution for giving access to their experimental work and data.

Of the students aiding in this work, particular mention is due to Messrs. Hutchins, White, Howland, Thomas and Childers, for their efforts.

I. Introduction

The subject of the stability of thin plates first became of practical importance in the fields of naval architecture and civil engineering. In naval architecture, the designer was interested in the failure of the side plates of a ship when they were subjected to normal and shearing forces in the plane of the plates. In this case, the problem was laso complicated for certain parts of the structure by the addition of the water pressure acting normal to the plane of the plate. The civil engineer faced a similar problem when desiguing large plate girders in which other dimensions of the web were very large in comparison to the thickness of the material used. These beams were subjected to loads which caused tension, compression, and shear loads which acted in the plane of the web, and it was the desiguer's problem to so construct his beam that buckling of the web did not take place.

In both of the above cases, failure was considered to have occurred when the plate suffered any appreciable deformation in a direction perpendicular to its plane; since any loading above this "critical load" caused a rapid increase in the deformation in a direction parallel to the plane of the sheet. This large deformation, if accumulated over a large structure such as a ship or bridge, would cause total displacements which could not be tolerated in the desing of such a structure.

When flat and curved sheet was first used in aircraft construction, the tendency was to design the sheets on the same basis as that used previously, i.e. on the

basis of the stability limit or the critical buckling load. This buckling load, however, was very low for the thin materials that were used in aircraft construction and this critical load induced stresses in the material which were far below the stresses that would cause permanent deformation in the sheet.

It was also noticed that if such thin sheet metal panels were loaded above the stability limit they continued to carry a certain amount of increased load without suffering any permanent deformation. Consequently there arose the second problem, that of ddetermining the maximum permissible load before the sheet suffered a permanent deformation, or before the stresses reached the elastic limit of the material at any point.

Because of the loading conditions of airplane structures, such conditions as indicated above are quite permissible. The normal flying or landing loads on an airplane are usually quite low compared to the loads which may be applied under extreme conditions for short periods of time. Consequently it may be possible to design the stressed sheet of such a structure so that it is in the unbuckled state for normal load conditions and can carry considerable larger loads in the buckled state when subjected to extreme conditions. In other words, the ultimate design load should be based on the ultimate load carrying capacity of the sheet rather than upon the load at which the sheet reaches the stability limit.

The determination of the elastic stability limit of flat sheet members has been made theoretically and checked experimentally by a number of authors. The first

theoretical treatment was made by Bryan (Reference 1) and his method, or other methods giving the same results, are given in a number of texts and papers on the theoretical treatment of elasticity. (References 2, 3, 4, and 5, and others). One method of treatment and the result obtained is given in Part II of this paper.

The treatment of the ultimate load beyond the stability limit is quite recent. It had been obtained experimentally a number of times but was first considered seriously in a publication of Newell's (Reference 6) and in N.A.C.A. Report No. 356 (Reference 7) on work done at the Bureau of Standards. These authors made no attempt to give a theoretical treatment of the subject but only gave the experimental data in the hope that these results would be a guide to designers.

The first analytical attempt on this problem was made by von Karman, and it is this treatment and its expansion which forms the basic part of this paper. A semi-theoretical treatment has been made for flat sheets under edge compression in the plane of the sheet, and this theory has been checked by a large number of experiments. This has then been extended to cover the cases of flat sheets acting in connection with stiffeners and of curved sheets with and without stiffeners. Part of the experimental work has been done personally by the author, part of it taken from reports of work performed at other institutions, and part of it was performed at C.I.T. by graduate students in Aeronautics. Mention of authors and publications will be made as their work is discussed.

II. The Stability Limit

In giving this discussion on the stability limit, only one set of boundary conditions will be considered in order to give a background for future work. The method is quite general, however, and different boundary conditions can be used in the general differential equation for other special cases.

Consider a plane plate lying in the XY-plane, of thickness "t" and dimensions "a" and "b" parallel to the X and Y directions respectively. This sheet is subjected to a compression load parallel to the Y-axis which gives a uniform stress σ distributed along the edges $y = 0$, and $y = b$. See Fig. 1. All edges of the sheet will be considered to be simply supported. Then, if the Z-axis is perpendicular to the sheet, the general differential equation

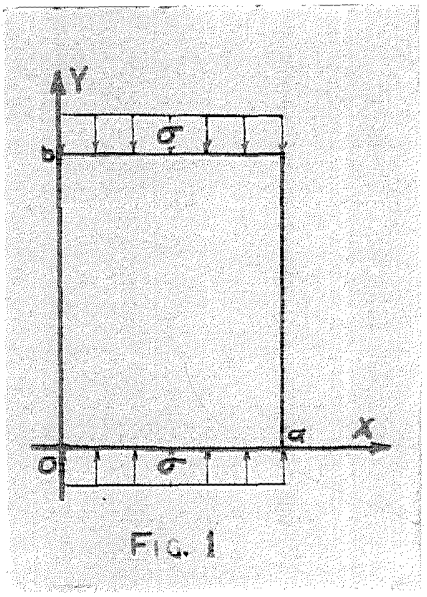

Fig. 1

is:

$$\frac{t^2E}{12(1-\mu^2)}\Delta\Delta z = \sigma_x\frac{\partial^2 z}{\partial x^2} + \tau_{xy}\frac{\partial^2 z}{\partial x\partial y} + \sigma_y\frac{\partial^2 z}{\partial y^2} \qquad (1)$$

and, since $\sigma_x = \tau_{xy} = 0 \qquad \sigma_y = -\sigma$

$$\frac{t^2E}{12(1-\mu^2)}\Delta\Delta z = -\sigma\frac{\partial^2 z}{\partial y^2} \qquad (2)$$

which gives the differential equation for this particular stress state as:

$$\frac{t^2E}{12(1-\mu^2)}\left[\frac{\partial^4 z}{\partial x^4} + 2\frac{\partial^4 z}{\partial x^2\partial y^2} + \frac{\partial^4 z}{\partial y^4}\right] + \sigma\frac{\partial^2 z}{\partial y^2} = 0 \qquad (3)$$

For the case of simply supported edges, "z" can be given by an equation of the form:

$$z = z_0 \sin \frac{n\pi x}{a} \sin \frac{m\pi y}{b} \tag{4}$$

where "m" and "n" are positive integers. Equation (4) satisfies the boundary conditions

$$z = 0, \quad \frac{d^2 z}{dx^2} = 0 \quad \text{at} \quad x = 0, a$$

$$z = 0, \quad \frac{d^2 z}{dy^2} = 0 \quad \text{at} \quad y = 0, b$$

Making the required differentiations, and putting the values into equation (3) we get, after dividing through by

$$z_0 \sin \frac{n\pi x}{a} \sin \frac{m\pi y}{b}$$

the equation

$$\frac{t^2 E}{12(1-\mu^2)} \left[\left(\frac{n\pi}{a}\right)^4 + 2\pi^4 \left(\frac{nm}{ab}\right)^2 + \left(\frac{m\pi}{b}\right)^4 \right] - \sigma \left(\frac{m\pi}{b}\right)^2 = 0 \tag{5}$$

which can be solved for σ, yielding

$$\sigma = \frac{\pi^2 E t^2}{12(1-\mu^2)} \left(\frac{b}{m}\right)^2 \left[\left(\frac{n}{a}\right)^2 + \left(\frac{m}{b}\right)^2 \right]^2 \tag{6}$$

This value is obviously a minimum when n = 1, although this is not true of "m". Putting in n = 1, we finally get

$$\sigma_{min} = \frac{\pi^2 E t^2}{12(1-\mu^2)} \left(\frac{b}{m}\right)^2 \left[\left(\frac{1}{a}\right)^2 + \left(\frac{m}{b}\right)^2 \right]^2$$

$$= \frac{\pi^2 E t^2}{12(1-\mu^2) a^2} \left[\frac{b}{ma} + \frac{ma}{b} \right]^2$$

$$= k \frac{\pi^2 E t^2}{12(1-\mu^2) a^2} \tag{7}$$

where

$$k = \left[\frac{b}{ma} + \frac{ma}{b} \right]^2 \tag{8}$$

A plot of K against the b/a ratio is given in Fig. 2. This family of curves indicates that the critical buckling stress is a minimum when the sheet has a length which is an even multiple of the width. Also, since "m"

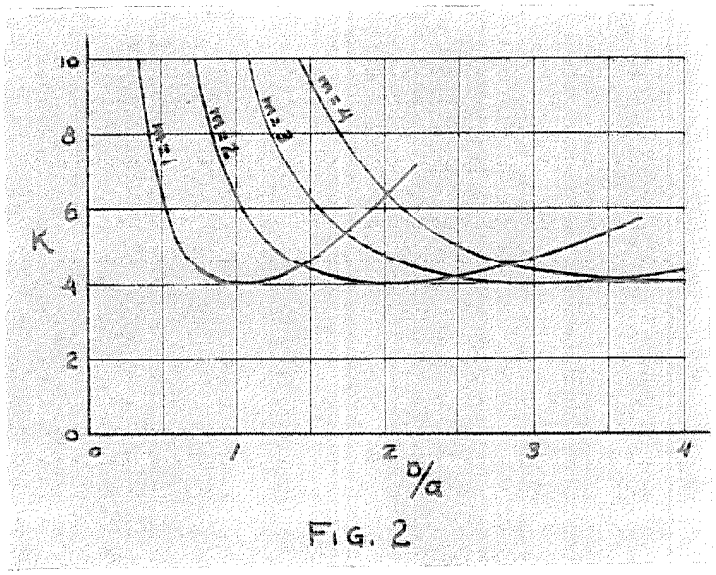

FIG. 2

gives the number of half waves in the Y direction, these curves indicate that the buckling tends to give nodal lines forming squares. The wave form in the X direction is one half-wave since n = 1 gave the minimum value for the stress.

The envelope of minima is given in Fig. 3, and this is the curve of K against the b/a ratio which is used for design. For all b/a ratios greater than 1.0 it is usually sufficiently accurate to consider that K = constant = 4.0.

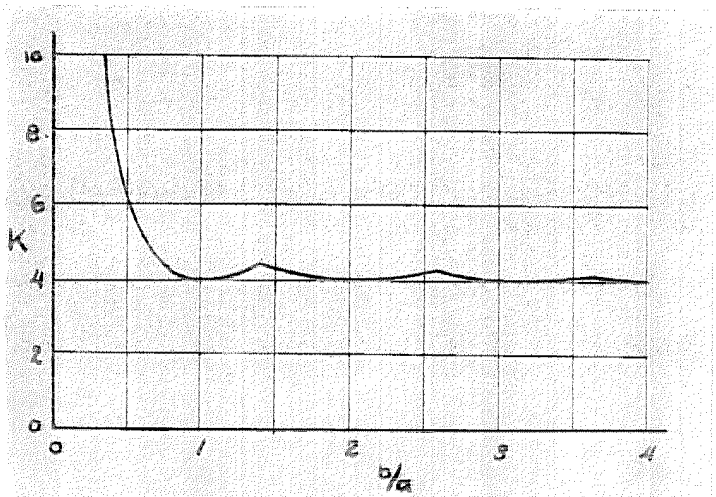

FIG. 3

This method of calculating the allowable load for sheet material proved very satisfactory for plates of the thickness used in naval and civil engineering as it was possible to obtain stresses reasonable close to the elastic limit of the material with quite large plates. For example, a sheet of structural steel $\frac{1}{8}$" thick could be used up to 30" wide and of any length without having the buckling stress fall below the elastic

limit (30,000 lbs./sq.in.) of the material.

It will be noticed, however, that the buckling stress falls off proportional to the square of the thickness and that the allowable width for a given stress decreases directly as the thickness of the material. For this reason, difficulty was encountered when the method was applied to the design of aircraft structures where the thicknesses of the material used lie in a range of from 0.012 to 0.120 inches, and may, for the case of stainless steels go down to a few thousandths of an inch.

Take, for an example, a simply supported panel of duralumin with a thickness of 0.040" under a compressive load. To get the buckling stress up to the elastic limit, say 40,000 lbs./sq.in., the width of the panel should not exceed

$$a = \sqrt{\frac{4\pi^2 E t^2}{12(1-\mu^2)\sigma}} = \sqrt{\frac{4\pi^2 \times 10^7 \times .040^2}{12(.91)\,40000}} = 1.2"$$

for any b/a ratio equal to, or greater than 1.0. This obviously means that numerous stiffeners must be used in order to break up the sheet into a large number of very narrow panels. This leads to an expensive and difficult construction which would not be used merely from an economic standpoint.

If a panel of the same material is made 4" wide, the buckling stress falls off to

$$\sigma = \frac{4\pi^2 \times 10^7 \times .040^2}{12 \times .91 \times 16} = 3610 \text{ lbs/sq.in.}$$

which is much too low for economical design. If the load on this panel is increased after buckling takes place, an average stress of over 7,000 lbs./sq.in. can be reached

before any permanent deformation takes place. Although this last stress is still far below the elastic limit of the material, the increase is important enough to be given serious consideration for thin sheet metal panels. Part III will consider this increase in allowable stress above the stability limit in detail.

III. Flat Sheet Panels Beyond the Stability Limit. First Approximate Theory.

Upon an investigation of the experimental work performed by the Bureau of Standards on flat sheet in compression (References 6 and 7), two rather striking facts were noted. The first item of importance was that the loads obtained gave stresses considerably above the critical buckling stress before any permanent deformation took place, and second, the value of the failure load was very nearly independent of the width of the specimen, when the specimen was wider than about four inches. The failure load seemingly depended only upon the elastic properties of the material and the square of the thickness of the sheet.

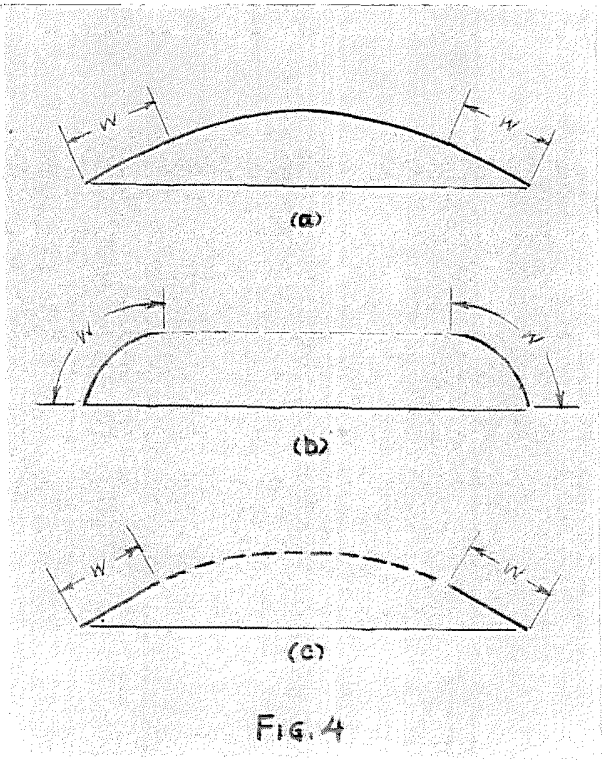

FIG. 4

From a purely physical analysis of the problem it seemed reasonable to assume that perhaps most of, or all of the load was carried by that part of the sheet near the edges which was supported and that the center of the sheet was carrying little or no load in the buckled state. In other words, an effective width of the sheet on each side was assumed to be carrying all of the load, in a manner similar to the assumption of an effective width for the design of T-beams with wide, thin flanges. This assumption was

theoretically in a recent paper (Reference 8) in the following manner:

After the critical buckling load has been reached, the sheet deforms in one half-wave in the direction perpendicular to the applied load, as shown previously in Part II. See Fig. 4a. After the deformation had occurred, it was assumed by von Karman that an effective width "w" at the

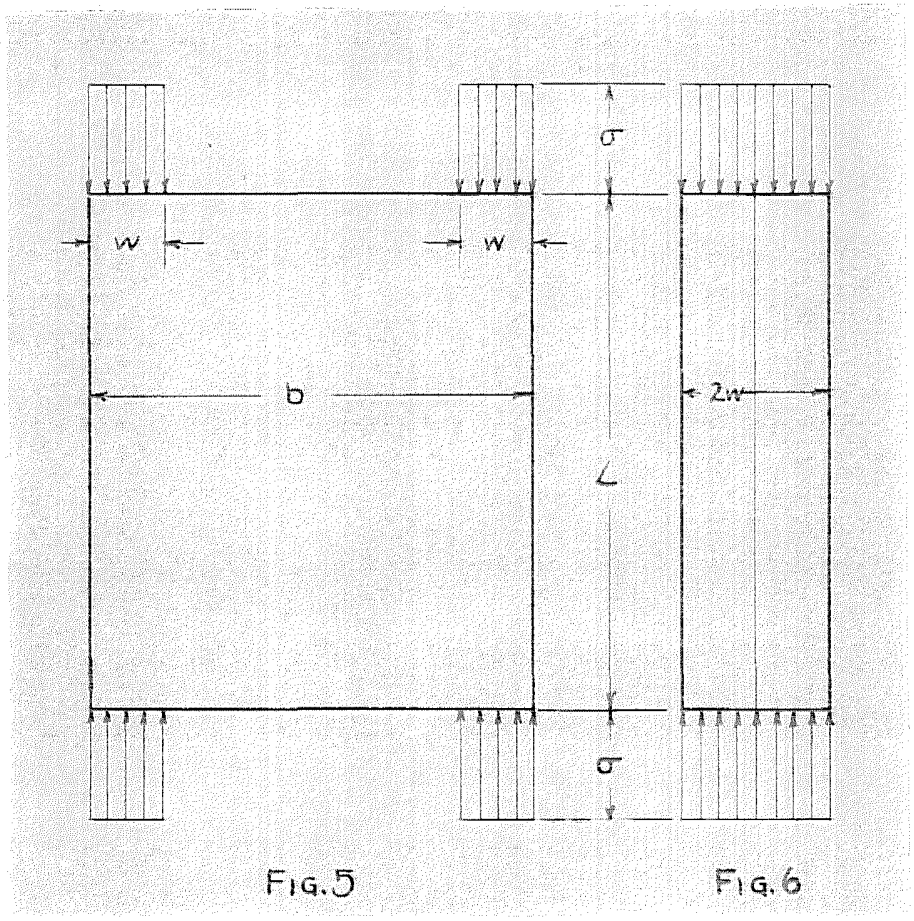

Fig. 5 Fig. 6

sides of the sheet carried the entire load and that the center of the sheet dropped out of action. See Fig. 5. In order to simplify calculations, there are two possible assumptions that can be made regarding the shape of the sheet in the region "w". The first of these, used by von Karman, assumes that in this region the plate deforms so that the tangents at the end of the two effective widths are parallel. See Fig. 4b. Thus, the center of the sheet can be elimin-

ated and the problem resolves itself into the failing stress of a plane sheet, with width 2w, length L, acted upon by a compressive stress σ. Then, if we use the method of Part II, the equation of the stress state corresponds to equation (3)

$$\frac{t^2E}{12(1-\mu^2)}\left[\frac{d^4z}{dx^4}+2\frac{d^4z}{dx^2dy^2}+\frac{d^4z}{dy^4}\right]+\sigma\frac{d^2z}{dy^2}=0 \qquad (3)$$

and equation (4) becomes

$$z = z_0 \sin\frac{\pi x}{2w}\sin\frac{\pi y}{l} \qquad (9)$$

where a = 2w and b/m = l = the half-wavelength of the deformation. The value of "n" in equation (4) is taken as unity since it was previously found that this gives the minimum value of the critical stress. Putting (9) into (3) we obtain:

$$\frac{Et^2}{12(1-\mu^2)}\left[\frac{\pi^4}{16w^4}+\frac{\pi^4}{2l^2w^2}+\frac{\pi^4}{l^4}\right]-\frac{\pi^2}{l^2}\sigma=0$$

or

$$\sigma=\frac{\pi^2Et^2}{12(1-\mu^2)}\left[\frac{l}{4w^2}+\frac{1}{l}\right]^2 \qquad (10)$$

To find the minimum of σ, the critical stress, we differentiate with respect to l and equate to zero. This gives,

$$\frac{1}{4w^2}-\frac{1}{l^2}=0$$

$$l = 2w$$

from which

$$\sigma_{critical}=\frac{\pi^2Et^2}{12(1-\mu^2)w^2} \qquad (11)$$

solving this for the effective width we get

$$w=\frac{\pi}{\sqrt{12(1-\mu^2)}}\sqrt{\frac{E}{\sigma}}\,t \qquad (12)$$

and the total load carried by the sheet is equal to

$$P_{TOT}=2wt\sigma=\frac{2\pi}{\sqrt{12(1-\mu^2)}}\sqrt{E\sigma}\,t^2 \qquad (13)$$

The maximum load possible before permanent deformation takes place is determined when $\sigma = \sigma_y$ = the yield point of the material. Thus

$$P_{max} = \frac{2\pi}{\sqrt{12(1-\mu^2)}} \sqrt{E\sigma_y}\, t^2 \tag{14}$$

$$= C_f \sqrt{E\sigma_y}\, t^2 \tag{15}$$

where

$$C_f = \frac{2\pi}{\sqrt{12(1-\mu^2)}} \tag{15a}$$

It might also be assumed that the effective width acts as a sheet simply supported on three sides with the fourth side free (Fig. 4c). This assumption has been carried out by Donnell (Reference 8) and he arrives at an equation for the maximum total load of the same form as (15). Donnell's equation is

$$P_{max}' = C_f' \sqrt{E\sigma_y}\, t^2 \tag{16}$$

where

$$C_f' = \sqrt{\frac{2}{1+\mu}} \tag{16a}$$

The above methods indicated that the correct procedure was being followed since they gave the ultimate load as a function of the elastic properties of the material, the square of the thickness of the material, and indicated that the load was independent of the width of the specimen. Considering the value of μ for normal aircraft material (metal) to be equal to 0.3, equations (15) and (16) give us

$$P_{max} = 1.91 \sqrt{E\sigma_y}\, t^2$$

$$P'_{max} = 1.24 \sqrt{E\sigma_y}\, t^2$$

respectively, and one would expect to find that the exper-

imental values would lie somewhere between these values since they are obviously the limiting cases. The experi-

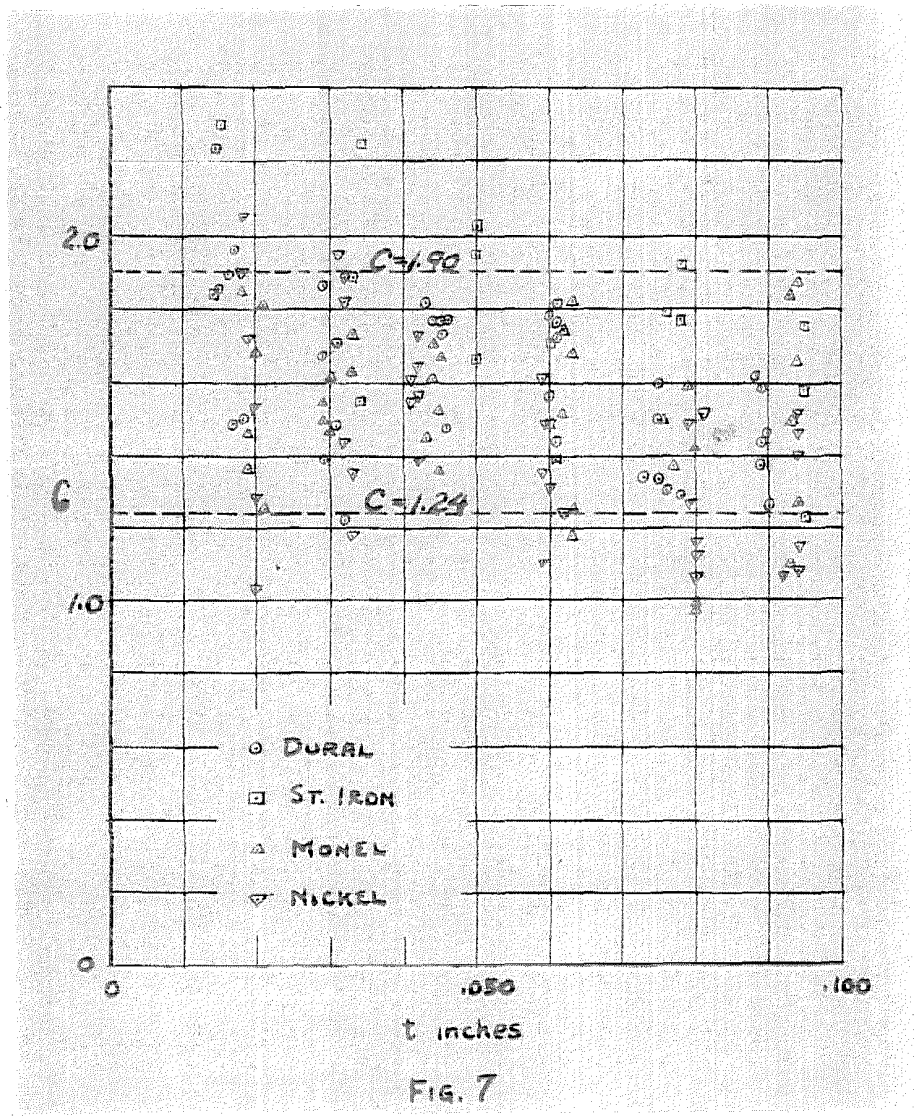

FIG. 7

mental values of C_f, calculated from the experimental loads found in Reference 7 are shown plotted in Fig. 7, and it is seen that nearly all (83%) of the experimental values for C_f do lie within the range indicated by the above calculations.

In order to more closely check the theoretical work an experimental program was started at the California Institute of Technology in the Guggenheim Aeronautical Laboratory. It was felt that certain faults of the testing equipment used previously invalidated some of the experimental results and

consequently an effort was made to eliminate these faults as much as possible in the testing equipment designed at C.T.T.

IV. Experimental Apparatus and Results of First Experimental Tests.

The testing machine used is shown by two sketches

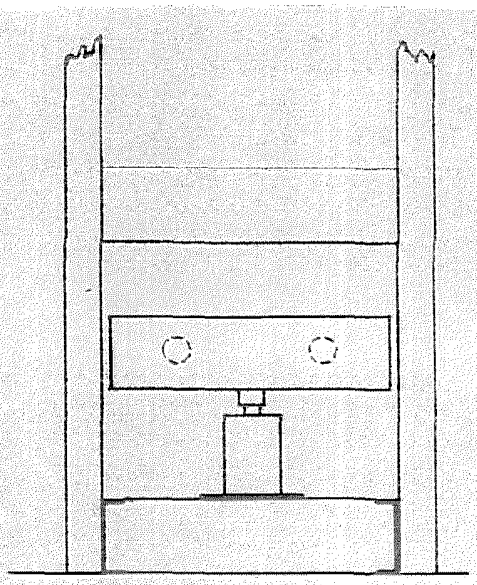

FIG. 8

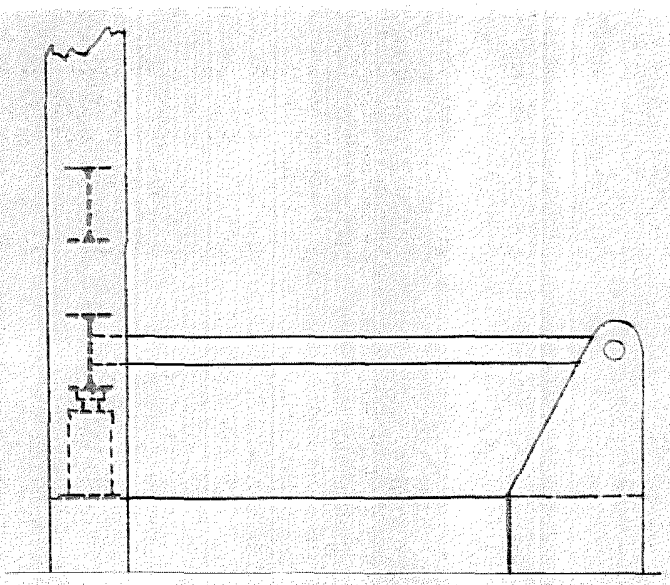

FIG. 9

in Figs. 8 and 9, and Fig. 10 shows a photograph of the machine in use. The upper head of the testing machine consists of a ten inch I-beam fastened to two upright ten inch channels, and the lower, moving head of the machine is a similar ten inch I-beam pivoted on ball bearings, with a lever arm of seven feet. This type of design was used so as to eliminate any friction which might be introduced from vertical guides. The heavy upper and lower beams were used in order to eliminate any deflection of the testing heads under

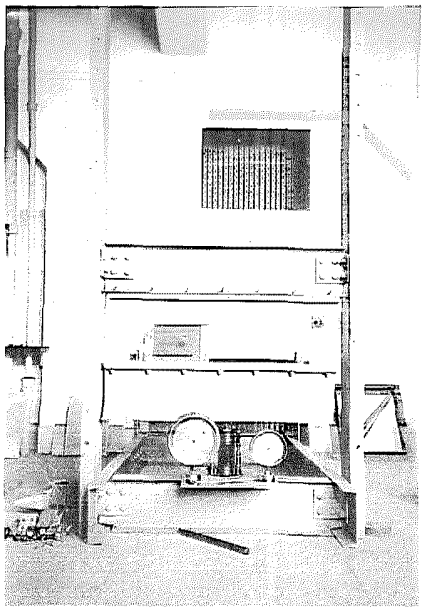

Fig. 10

load, which would tend to distort the load distribution over the edges of the specimen. The horizontal motion of the lower beam, being approximately 0.01 inch for every inch of vertical motion, could be neglected, for the vertical motions obtained in the experiments were in general less than a quarter of an inch.

The load was applied by means of a seven and one-half ton hydraulic jack and the values of the loads were determined by means of a high-range and a low-range pressure gauge. See Fig. 11. The low-range gauge read from 0-2000 pounds and the high-range gauge read from 0-20,000 pounds. These gauges were periodically calibrated against a standard type testing machine.

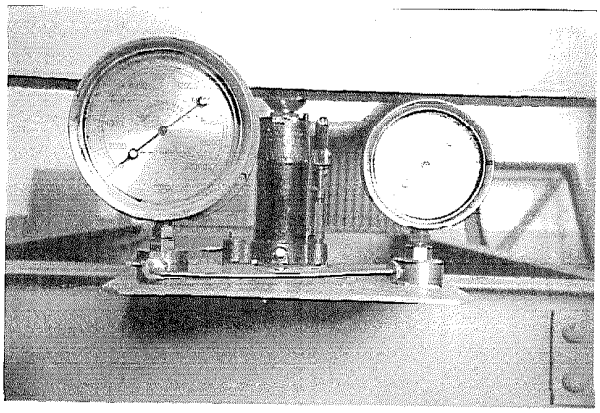

Fig. 11

The surfaces of the I-beams next to the specimens were faced with a strip of heavy cold-rolled steel having a 120° V-groove running lengthwise down the center of the beam. These two V-grooves could be accurately aligned, one above the other, by means of adjustments on the testing machine. The sides of the specimens were also supported in V-grooves, in this case 30°, which could be adjusted for any

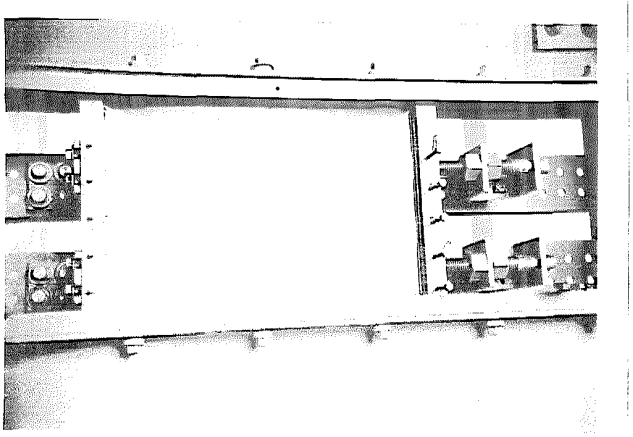

Fig. 12

width of sheet desired and which could also be adjusted so that they were in the plane of the top and bottom grooves. A photograph of the edge supports first used is shown in Fig. 12. In this manner, the specimen was as nearly as possible simply supported on all four edges with a compression load on the upper and lower edges acting in the plane of the sheet.

The first series of tests was run on specimens which were all 12" long and which varied in width from 1 to 19 inches. Materials used were, 17ST Dural, soft steel sheet, aluminum, and brass, with a thickness range of from 0.012 to 0.067 inches. Since the Karman analysis (Part III) indicated that the total load carried was a function of the Young's modulus, the yield point, and the thickness of the material, a wide range of these values was desired in order to check the equation, even though some of the materials tested were not practical from the standpoint of airplane structural materials. It was also expected that for very large and very small values of the length-breadth ratio this equation would break down, so a wide range of widths was used in order to establish the limits of usefulness of the equation.

The material was ordered crated and shipped flat when purchased and was used as received, rejecting however, any specimens which showed any appreciable curvature or defects. The ends were sheared square and the loaded edges of the specimens were made semi-circular as there was a tendency for flat edges to ride on one side of the upper and lower V-grooves, thereby putting a shock load on the specimen and causing it to fail prematurely. A number of scattered one inch wide specimens were taken close to the larger compression

specimens and these were used as tension specimens for the determination of the elastic properties of the material. The elastic properties were determined in a 3000 pound Reihle tension machine, elongations being measured with balanced Huggenberger tensiometers. See Fig. 13.

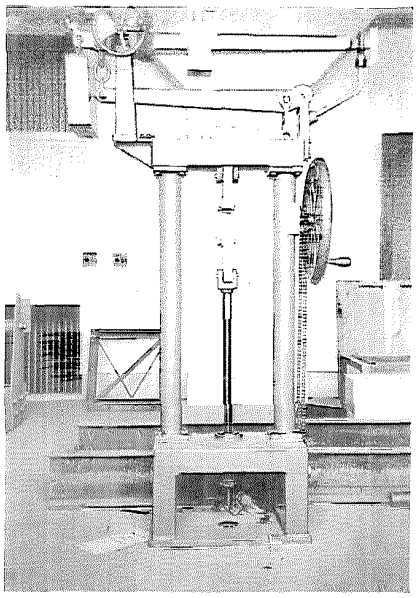

Fig. 13

The compression tests were run on each specimen and the value of the ultimate load in compression was tabulated. From this, using equation (15), the value of C_f could be determined, since E and σ_y were given by the stress-strain curve of the material and "t" could be measured. For the determination of the experimental values of C_f, σ_y was taken as the point on the stress-strain curve of the material at which the curve first departed from a straight line. This definition of σ_y was later modified, but at this time it was considered suitable to check the equation.

Table I, columns 1-9, show the results of this first set of experimental tests. It may be noticed that the values of C_f in this table are not widely different, considering the wide range of the experimental variables, however there seemed to be enough difference to justify a further analysis in order to determine whether or not this difference was due to experimental inaccuracies or whether C_f was some function of the experimental variables. Consequently a closer investigation of the probable stress distribution was carried

out and a second approximation to the probable ultimate load carried by such a specimen was made.

V. Second Approximate Theory

The first assumption made in determining the ultimate load that could be carried by a thin sheet panel in compression was that the center of the sheet carried no load and that the edge regions supported the entire load carried by the sheet. However, an investigation of the action of a sheet during loading shows that this assumption needs to be modified in order to more closely approach the actual load distribution over the loaded edges.

At first, the sheet remains in its original plane form as the load is applied. At a certain load, the critical buckling load, which can be determined by the equations derived in Part II, the sheet buckles in a wave-form which is a function of the dimensions of the sheet. As the loading is continued, the edges remain restrained and continue to carry increasing load. The center portions of the sheet, being in the buckled state, can carry little or no increase in load, however they still carry the stress corresponding to the critical buckling load on the panel. The second approximation to the ultimate compressive load is based on the above assumption, i.e. that the center portion of the sheet carries a stress corresponding to the critical buckling stress of the given panel and that the edges of the sheet carry a stress σ distributed over the effective width "w".

Consider a thin sheet panel of length L, width b, and thickness t, made of material with a Young's modulus E, and a yield point σ_y ; simply supported on all four edges and subjected to a compression load on the upper and lower edges. Assume a load distribution as in Fig. 14, in which the

regions over the effective width "w" on each side carry a uniformly distributed stress σ and the center portion of the sheet, of width (b - 2w), carries the critical buckling stress of the sheet, σ_b . Using the Karman assumption, equation (12) gives the value of "w" as

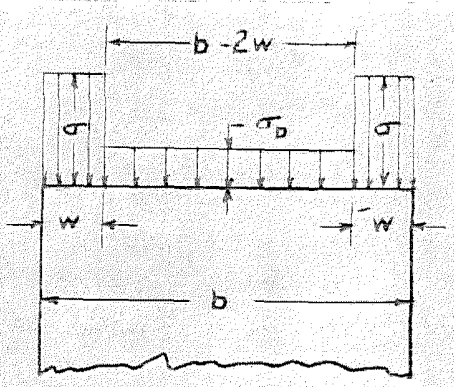

FIG. 14

$$W = \frac{\pi}{\sqrt{12(1-\mu^2)}} \sqrt{\frac{E}{\sigma}}\, t \qquad (12)$$

and the buckling formula, equation (7) gives

$$\sigma_b = K \frac{\pi^2}{12(1-\mu^2)} \frac{E t^2}{b^2} \qquad (7)$$

Let

$$\alpha = \sqrt{12(1-\mu^2)} \qquad (17)$$

then

$$W = \frac{\pi}{\alpha} \sqrt{\frac{E}{\sigma}}\, t \qquad (12a)$$

and

$$\sigma_b = K \frac{\pi^2}{\alpha^2} \frac{E t^2}{b^2} \qquad (7a)$$

where K is the constant depending upon the L/b ratio given in Fig. 3.

The total load carried by the ends is given by:

$$P = 2wt\sigma = \frac{2\pi}{\alpha} \sqrt{E\sigma}\, t^2 \qquad (18)$$

and the total load carried by the center section is :

$$P' = (b-2w)t\sigma_b = \frac{K\pi^2}{\alpha^2 b} E t^3 \left(1 - \frac{2\pi}{\alpha} \sqrt{\frac{E}{\sigma}} \frac{t}{b}\right) \qquad (19)$$

By adding the two, we get the total load carried by the combination as:

$$P_{Tot} = P + P' = \sqrt{E\sigma}\, t^2 \times \frac{2\pi}{\alpha} \left[1 + \frac{K\pi}{2\alpha} \sqrt{\frac{E}{\sigma}} \frac{t}{b} - \frac{K\pi^2}{\alpha^2} \frac{E}{\sigma} \frac{t^2}{b^2}\right] \qquad (20)$$

Letting

$$\lambda = \sqrt{\frac{E}{\sigma}}\,\frac{t}{b} \tag{21}$$

we get

$$P_{TOT} = \sqrt{E\sigma}\,t^2 \times \frac{2\pi}{\alpha}\left[1 + \frac{K\pi}{2\alpha}\lambda - \frac{K\pi^2}{\alpha^2}\lambda^2\right] = C_f\sqrt{E\sigma}\,t^2 \tag{20a}$$

where

$$C_f = \frac{2\pi}{\alpha}\left[1 + \frac{K\pi}{2\alpha}\lambda - \frac{K\pi^2}{\alpha^2}\lambda^2\right] = f(\lambda, K, \mu) \tag{22}$$

As before, the maximum load which can be carried by such a sheet is found when $\sigma = \sigma_y$. Substituting this value in equation (20a) we obtain:

$$P_{max} = \sqrt{E\sigma_y}\,t^2 \times \frac{2\pi}{\alpha}\left[1 + \frac{K\pi}{2\alpha}\lambda_y - \frac{K\pi^2}{\alpha^2}\lambda_y^2\right] = C_f\sqrt{E\sigma_y}\,t^2 \tag{20b}$$

in which

$$\lambda_y = \sqrt{\frac{E}{\sigma_y}}\,\frac{t}{b} \tag{23}$$

Poisson's ratio, μ, can be taken as a constant with the value 0.30 and this then leaves C_f as a function of λ and K. Fig. 3 indicates that K = 4.0 is a good constant value to use whenever the L/b ratio is greater than unity and that it is conservative to use this value for K for all values of L/b. Taking then, K = 4.0 and μ = 0.30, which gives a value of α = 3.29, we get for C_f:

$$C_f = \left[1.91 + 3.65\lambda - 6.96\lambda^2\right] \tag{24}$$

which is shown as Curve I in Fig. 15. This curve should hold up to the time when the two effective widths would join, or when (b - 2w) = 0. From this point on, the failure would be purely a yield point failure and the total load carried would be equal to

$$P = bt\sigma = C_f'\sqrt{E\sigma}\,t^2 \tag{25}$$

where, in this case,

$$C_f' = \frac{b t \sigma}{\sqrt{E\sigma}\, t^2} = \sqrt{\frac{\sigma}{E}}\,\frac{b}{t} = \frac{1}{\lambda} \qquad (26)$$

This is shown as Curve II in Fig. 15

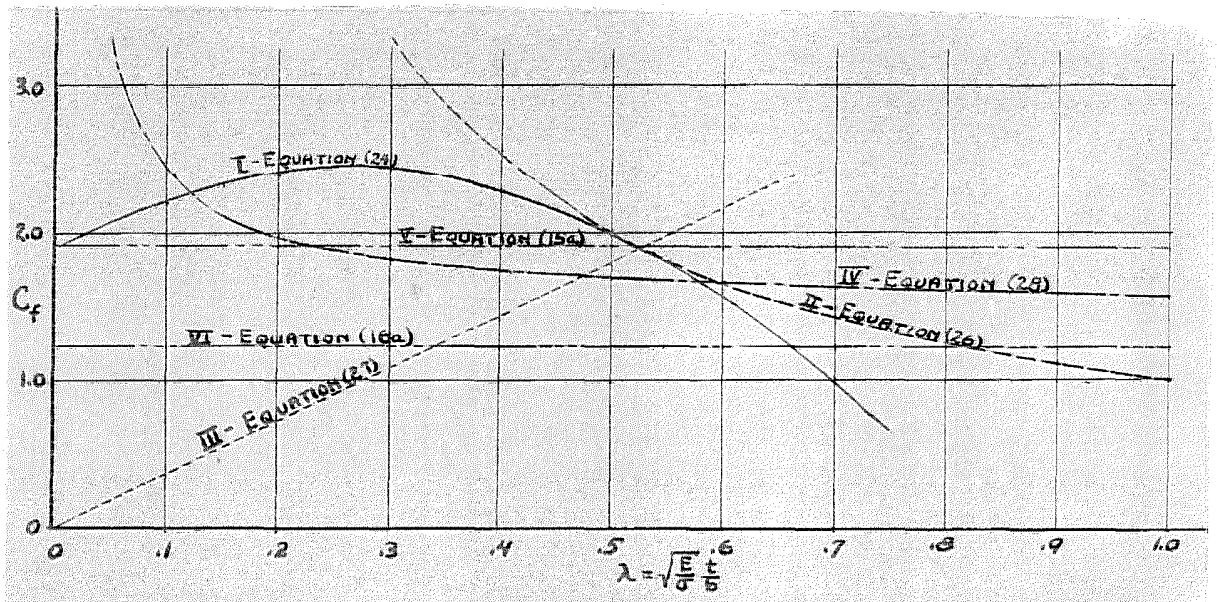

Fig. 15

In order to show the theoretical increase in load which can be carried after elastic buckling takes place, we will rewrite the buckling load equation in the form of equation (15). The load carried at buckling is given by

$$P_b = b t \sigma_b = b t \left[K \frac{\pi^2}{\alpha^2} \frac{E t^2}{b^2} \right] = K \frac{\pi^2}{\alpha^2} E \frac{t^3}{b}$$

and, putting it into the form

$$P_b = C_f'' \sqrt{E\sigma}\, t^2$$

we get for C_f''

$$C_f'' = K \frac{\pi^2}{\alpha^2} \sqrt{\frac{E}{\sigma}}\,\frac{t}{b} = K \frac{\pi^2}{\alpha^2} \lambda = 3.62\lambda \qquad (27)$$

for the region in which $K = 4.0$ and $\alpha = 3.29$. This gives a straight line as shown in Curve III in Fig. 15. The difference between Curve I and Curve III is proportional to the amount of load carried after buckling takes place.

In a recent paper by Cox of England (Reference 9)

a slightly different method was used to calculate the allowable compressive strength of flat sheet, using very nearly the same initial assumption as used in this second approximation and a formula was obtained which could be put into the form

$$P = C_f''' \sqrt{E\sigma}\, t^2$$

where

$$C_f''' = \left[1.52 + 0.09\,\frac{1}{\lambda}\right] \qquad (28)$$

and where λ is defined as in the above derivation. This curve is shown as Curve IV in Fig. 15. Also, for reference, the two values of C_f found from the first approximate theory are shown as Curves V and VI.

Fig. 16 shows the experimental values of C_f from

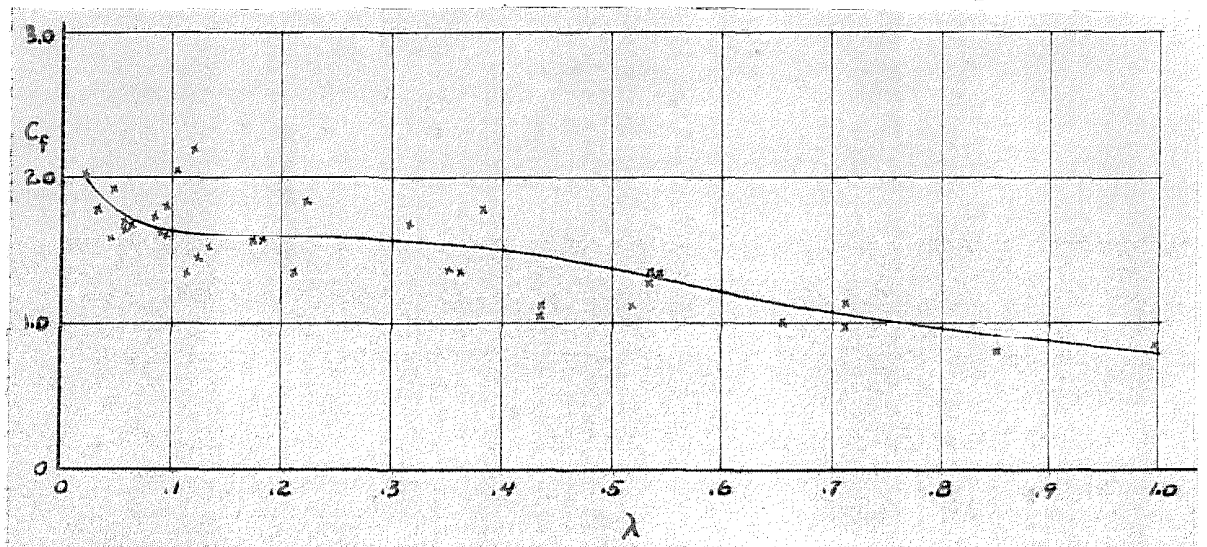

FIG. 16

Table I plotted against λ. This plot shows that there is a definite relationship between C_f and λ even though the curve shown, which is taken as the mean curve through the plotted points, does not agree with any of the theoretical curves in Fig. 15.

This first set of experiments answered two very important questions -- first that the total compression load that could be supported by a flat panel could be given by the equation

$$P = C_f \sqrt{E\sigma_y}\, t^2$$

and, second, that the coefficient C_f was a function of the parameter

$$\lambda = \sqrt{\frac{E}{\sigma}}\ \frac{t}{b}$$

for a wide range of materials with different elastic properties. There remained one variable that had not been investigated, the effect of the length of the specimen on the value of the flat sheet constant. Also, a more accurate determination of the exact shape of the C_f vs. λ curve was desired. For these reasons a second series of tests were made on flat sheet panels. With the fact established that the value of C_f could be plotted as a function of λ, a much larger series of panels were designed in order to better determine this dependance.

In order to obtain a number of points over the whole range of possible values of λ a series of specimens were chosen from 0.064" and 0.032" 17ST Dural and from 0.026" and 0.012" steel with widths chosen to cover the range from $\lambda = 0$ to $\lambda = 1.0$. Since Table I had shown that the value of C_f was more doubtful for small values of λ the concentration of experimental points was made greater as λ decreased. This lead to specimens ranging from 0.8" to 15.0" in width.

For the determination of the dependance of C_f on the length of the panel, seven different lengths of specimens

were chosen ranging from 3" to 21" in steps of 3". This gave a total of 105 specimens which, with a few additional panels tested, covered the ranges of variables as indicated

t from 0.012 to 0.064 inches

b from 0.8 to 15.0 inches

L from 3 to 21 inches

L/b from 0.20 to 25.0

λ from 0 to 1.0

For this series of tests new V-grooves were designed which were much more rigid than those used in the first group of experiments, support for the edges of the sheet being carried into the lower and upper V-grooves by means of auxiliary ground blocks. The lower blocks were made of thin sheets which were compressed as the lower head of the testing machine moved upwards. The load necessary to compress the spring leaves of these blocks was negligible compared to the total load carried by the panels and so was neglected.

The experimental results of these tests are given in Table II and plotted in Fig. 18. It can be seen from Fig. 18 that there is no great difference between the values of C_f for L/b ratios greater than 1.0. For the L/b ratios less than 1.0 there seems to be an increase in the value of C_f as L/b decreases as shown by the dotted curves. This is as would be expected as the stress carried by the center regions of the panel increases as the L/b ratio decreases from 1.0. However, for design purposes, it is felt that the use of the solid curve in Fig. 18 for all values of L/b will give good design values for the flat sheet coefficient. This curve has been replotted to a larger scale in Fig. B-1 in Appendix B.

In Table II the value of σ_y was taken as that point on the stress-strain curve of the material which corresponded to a 0.2% permanent elongation of the material. This was done, first to agree with the definition of the yield point given in the Army design requirements, and second because the use of this value seemingly gave less scatter to the experimental points. This scatter was particularly noticeable in materials with a stress-strain curve which departed slowly from a straight line, failure seemingly being retarded until a stress had been reached which was considerably beyond the proportional limit of the material. A discussion of the shape of the experimental curve follows in the next section.

VI. Discussion of Results of Tests on Flat Panels.

Probably the most important result of all of the experiments performed on flat panels was the confirmation of the equations for flat sheet, equations (15) and (21). This

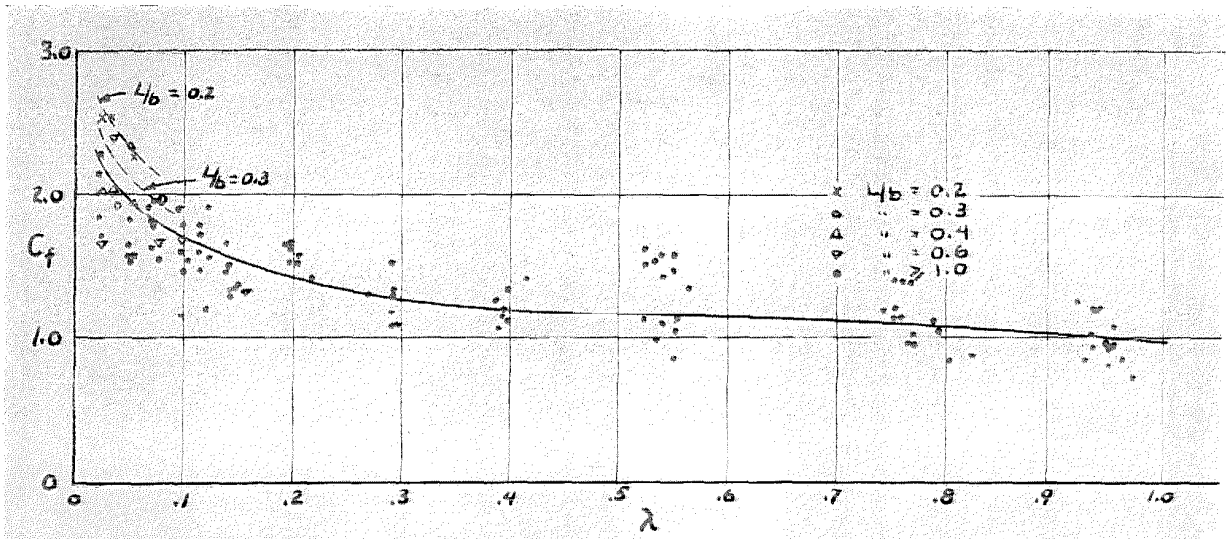

Fig. 18

was particularly fortunate since the whole theoretical discussion has been based on the assumption that the small deflection theories hold beyond the stability limit. This assumption has been made in the derivation of all of the curves in Fig. 15. Obviously, after the sheet has gone into the wave state, the only theoretical treatment that would be sound would be a treatment based on the theory of large deflections in which the stresses introduced from bending were considered as well as the stresses due to direct load. This treatment has been started by Donnell but as yet is not in a form that would make it applicable to the

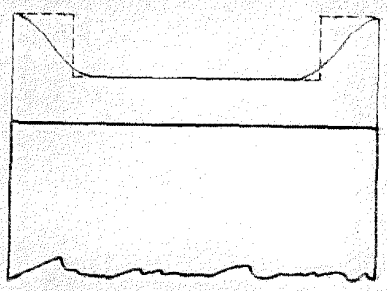
Fig. 17

confirmation of experimental results.

An investigation of the experimental curve of Fig. 18 indicates that it is below the theoretical curves of Fig. 15 for nearly all values of λ. From a purely physical reasoning the loading over the effective width "w" cannot be uniform as shown in Fig. 14, but the stress must be a maximum at the edges and drop off gradually to the buckling stress in the center as shown in Fig. 17. This means that the total load would be lower than that predicted by the second approximation. The position of the experimental curve shows this to be correct except for very small values of λ.

The increase in the value of C_f at small values of λ is probably due to two effects. Small values of λ indicate that either t must be small or that b must be large. If b is large, giving a L/b ratio less than unity, the value of the constant K rises rapidly as shown in Fig. 3, and the value of the stress carried by the center portion of the sheet increases proportionally. That there is a tendency for C_f to increase for decreasing values of L/b is shown by the dotted curves in Fig. 18, however, this effect is so small that for design purposes it is felt that the use of the solid curve, neglecting the small effect of L/b is advisable.

There is another effect, however, which was first noticed when testing wide specimens of thin brass. Owing to the polished nature of this material, small waves were easily noticed and the buckling action was visible throughout the loading. Taking, for example, a sheet 12" long, 14" wide, and 0.016" thick, corresponding to a value of $\lambda = 0.025$, the buckling first started at a very low load and was in the form of one half-wave, as would be expected from the buckling

equation. This form continued until a load equal to approximately one-third of the failure load was reached and then the edges of the sheet buckled in the form of five half-waves. As the load was increased still further, these five half-waves moved out towards the center of the sheet and then finally a large number of small waves (twelve half-waves on one side and thirteen on the other) appeared on the edges, shortly after which the sheet failed. The specimen shown in Fig. 12 shows clearly the multiple wave form which thin, wide sheets go into. This multiple wave form can also be noticed in a number of the wider specimens shown in the photographs in Fig. 19.

The above action was observed for all of the wider panels tested and the effect seemed to decrease as the sheets became narrower. This would seem to indicate that for the wider sheets the distribution of stress on the loaded edges could not be accurately expressed even by the second method given above. The interaction of the different sets of waves probably gives a stiffening effect which is shown by the increase in the value of C_f as the value of λ decreases. A more careful investigation of the actual wave form of the sheet under load is being planned in order to see if it will not give a better idea as to the actual stress distribution across the loaded edges.

Fig. 19 shows a number of photographs of test panels taken after failure, in which the type of wave form can be clearly seen. Also, the more rigid edge supports for the edges of the sheet can be seen in these pictures.

FIG. 19

VII. Application to Curved Sheet Panels

The method of Part V. will now be expanded to cover the problem of the ultimate compressive strength of curved sheet panel without stiffeners.

Consider a simply supported panel of developed width "b", length "L", thickness "t", curved to a radius "R", and loaded with a compression load in the plane of the sheet and parallel to the axis of the cylindrical surface. See Fig. 20. Assume the Young's modulus of the material to be E and the yield point to be σ_y. Since the sides of the sheet are simply supported, they will undergo a stress condition similar to that found for the flat sheet, i.e. at failure the stress at the very edge will be σ_y and this stress will decrease as the center of the sheet is approached. However, for simplification, it will be assumed that the region very close to the edge will act as a flat sheet and will support a stress σ over an effective width "w", where "w" is obtained from the equation for flat sheet:

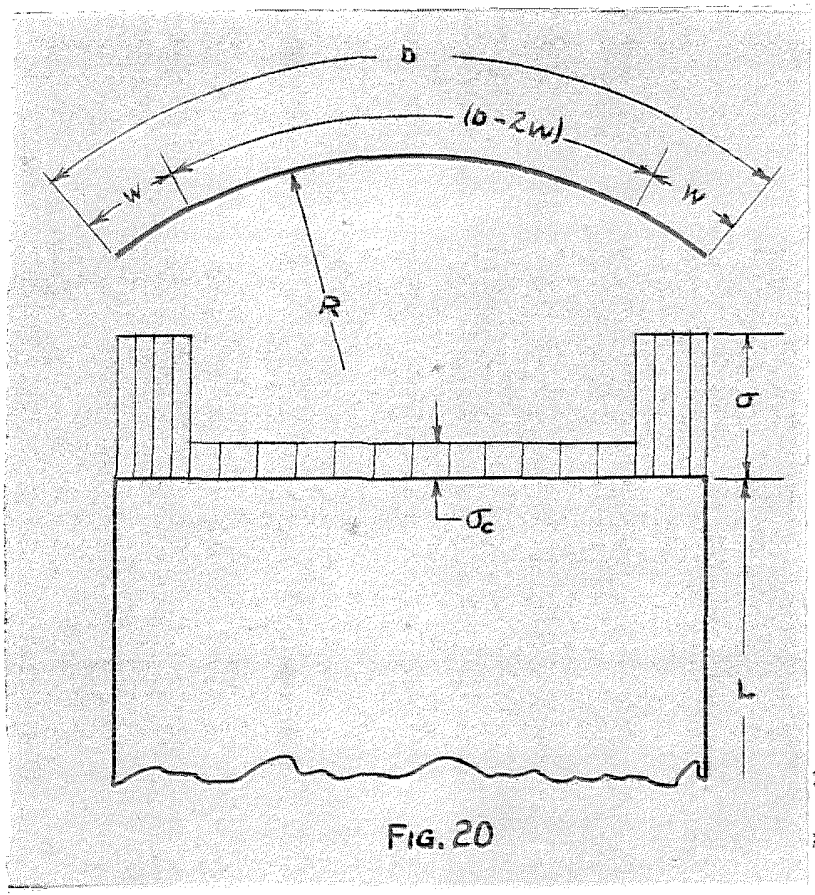

FIG. 20

$$w = \frac{C_f}{2}\sqrt{\frac{E}{\sigma}}\,t \tag{29}$$

where

$$C_f = f(\lambda) = f\left(\sqrt{\frac{E}{\sigma}}\,\frac{t}{b}\right) \tag{30}$$

as given in Fig. B-1, Appendix B.

The total load carried by the two side regions will then be

$$P = 2wt\sigma = C_f\sqrt{E\sigma}\,t^2 \tag{31}$$

The experimental work of Mossman and Robinson (Reference 10) indicated that the failing stress of circular cylindrical specimens could be closely approximated by the equation

$$\sigma_c = 0.3E\,\frac{t}{R} \tag{32}$$

and a recent paper by Redshaw in England (Reference 11) has shown theoretically that the same critical buckling stress should hold for a simply supported curved sheet panel as for a complete circular cylinder. The value of the coefficient in equation (32) also agrees with the compiled experimental data given in an N.A.C.A. Report by Lundquist (Reference 12).

For the case under discussion it will be assumed that the center of the panel acts as a cylindrical section under compression and will not carry any additional load after it has reached the stress σ_c; however, the failure of the panel as a whole will be retarded by the support at the sides which will enable the side regions to carry additional stress above the critical stress value for the center regions.

On the basis of the above discussion, it is as-

sumed that the stress distribution over a simply supported curved sheet panel is as follows:

a) Over a region of width "w" on each side, there is acting a stress σ_c.

b) Over the central region of width (b - 2w) there is acting a stress given by equation (32). See Fig. 20.

The load carried by the side regions is given by equation (31) and the load carried by the center is given by

$$P_c = (b-2w)\sigma_c t = b\sigma_c t - 2w\sigma_c t$$

$$= .3E\frac{bt^2}{R} - .3C_f E\sqrt{\frac{E}{\sigma}}\frac{t^3}{R} \qquad (33)$$

The total load is then given by

$$P_{TOT} = P + P_c = C_f\sqrt{E\sigma_y}\,t^2 + .3E\frac{bt^2}{R} - .3C_f\frac{Et^3}{R}\sqrt{\frac{E}{\sigma}} \qquad (34)$$

which, if put into the form used in flat sheet calculations, becomes

$$P_{TOT} = C\sqrt{E\sigma}\,t^2 \qquad (35)$$

where

$$C = \left[C_f + .3\sqrt{\frac{E}{\sigma}}\frac{b}{R} - .3C_f\frac{E}{\sigma}\frac{t}{R}\right] \qquad (36)$$

which can be put into the form

$$C = \left[C_f\left(1-.3\frac{E}{\sigma}\frac{t}{R}\right) + .3\sqrt{\frac{E}{\sigma}}\frac{b}{R}\right] = \left[C_f(1-.3\varepsilon) + .3\eta\right]$$

where

$$\varepsilon = \frac{E}{\sigma}\frac{t}{R} \quad \text{and} \quad \eta = \sqrt{\frac{E}{\sigma}}\frac{b}{R}$$

In this equation for C, C_f is a function of

$$\lambda = \sqrt{\frac{E}{\sigma}}\frac{t}{b}$$

so the equation can be written as a function of λ and η alone, as given below

$$\varepsilon = \frac{E}{\sigma}\frac{t}{R} = \frac{t}{b}\sqrt{\frac{E}{\sigma}} \times \frac{b}{R}\sqrt{\frac{E}{\sigma}} = \lambda\eta \qquad (38)$$

$$C = \left[C_f(1-.3\lambda\eta) + .3\eta\right] \qquad (39)$$

This value of C plotted against λ and η is given in Fig. B-2, Appendix B. It will be noticed in equation (39) that if the radius of the specimen is infinite, i.e. a flat plate, $\eta = \varepsilon = 0$, and $C = C_f$, which gives the trueexperimental value for the flat plate; since in equation (39) and Fig. B-2 C_f is taken from the value of C_f as a function of λ as determined experimentally. Thus, in Fig. B-2, the curve for $\eta = 0$ corresponds to sheets with infinite radius or flat sheet specimens.

The curves for the value of C are also limited by their intersection with the curve giving the yield point failure of the panel as a whole. This is shown in Fig. B-2 and points to the right of this curve indicate that the stress in the center of the sheet as given by equation (32) is higher than the yield point stress of the material and that the panel would fail as a yield point failure at a value of C given by the limiting curve.

During 1931-32 a large number of experiments were made at M.I.T by Newell and Gale on the strength of curved sheet panels (Reference 13). One series of experiments was made on curved unstiffened panels and another series was made with various sheet and stiffener combinations. The unstiffened panels were simply supported in V-grooves and were loaded in compression under conditions which closely approximated the conditions assumed in the above calculations. These experiments have been used to calculate the value of

C from the experimental value of the total load by the equation

$$C = \frac{P_{exp}}{\sqrt{E\sigma_y}\, t^2} \qquad (40)$$

in which it has been assumed that $E = 10^7$ and $\sigma_y = 36{,}000$ lbs./sq.in. The results of this calculation are given in Table III.

From Table III it can be seen that the above method of calculation gives a very good check on the values of the curved sheet constant as determined by experiment, and could be used directly for the calculation of the maximum compression load that could be resisted by a curved sheet panel without stiffeners. However, a closer inspection of the experimental and theoretical values seems to indicate that there is a consistent variation of the value of C with the length of the specimen, the shorter specimens giving higher, and longer specimens giving lower, values than are obtained by equation (39). Taking the average ratio between the theoretical value of C and that obtained by experiment for each length, we obtain

For L = 6" C(exp) = 1.1 C(theory)

L = 12" C(exp) = 1.0 C(theory)

L = 18" C(exp) = 0.9 C(theory)

There are two possible explanations of this variation with length, the first being that the stress σ_c is a function of the length of the specimen, since the last series of tests on flat sheet proved that there was no variation of importance in C_f with variations in length. This source of error, however, does not seem important as the value of σ_c has been checked for a large range of lengths of specimens and there has never been noticed any consistent variation.

The second possibility of error lies in the method of edge support used for the panels. The sides of the sheet were supported in V-grooves with an angle of 45° which is too large. These grooves initially hold the sheet in a straight line, but if any buckling takes place in the center of the sheet, the edges are free to move out of the grooves. This motion will allow the edge of the sheet to deflect perpendicular to the plane of the plate and to act as an Euler column with a restricted range of buckling. This would tend to decrease the load carried by the edge region and this buckling load would very likely be a function of the length of the column. An investigation of the stiffened sheet panels, discussed later, seems to indicate that the second source of error is the most probable.

On the basis of the above discussion, and on the results of the check with stiffened curved sheet panels, it is felt that the value of C obtained from equation (39) or Fig. B-2 can safely be used for design purposes.

VIII. Sheet Panels with Stiffeners.

Sheet panels are never used in the construction of an airplane simply supported as those of the experimental tests we have just been discussing, but always have stiffener shapes forming the boundaries of the panel. We are particularly interested then in determining the load that can be carried by a thin sheet panel to which are attached stiffeners running in the direction of the applied compression load.

For this determination a method suggested by Lundquist (Reference 14) is used. The effective width of the sheet is assumed to act with the stiffener section as a column under compression. This column will fail under a certain compressive stress σ_{st} which will be a function of the type of stiffener, the effective width of the sheet acting with it, the length, and the degree of end fixity of the column. For the determination of the effective width, the equation for flat sheets is used

$$w = \frac{C_f}{2}\sqrt{\frac{E}{\sigma}}\,t$$

in which $\sigma = \sigma_{st}$ and C_f is a function of λ where

$$\lambda = \sqrt{\frac{E}{\sigma_{st}}}\,\frac{t}{b}$$

It can readily be seen that the determination of the true value of σ_{st} can only be obtained by a series of approximations. This calculation is carried out in detail in Appendix A and consists in starting with some arbitrary value of σ_{st} e.g. the value of the failing stress of the stiffener with no sheet attached, calculating the effective sidth "w" using this value, determining the radius of gyration of the

combined sheet and stiffener section, and from this obtaining a second value of σ_{st} . This procedure is carried out until σ_{st} and "w" are compatible, which usually involves not more than three approximations. Then, the total load carried by a stiffened sheet panel (flat) is given by the sum of the loads carried by these sheet-plus-stiffener columns. This gives

$$P = \sum \sigma_{st} (A_1 + A_2) \tag{41}$$

where A_1 is the area of the stiffener, A_2 is the area of the sheet attached to the stiffener, and σ_{st} is the final calculated failing stress of the combined section.

In the case of curved sheet panels with stiffeners, the panels carry, in addition to the above load carried by that part of the sheet next to the stiffeners, a load in the center of the panel given by the equation

$$P' = \sigma_c (b - 2w) t \tag{42}$$

where σ_c is given by equation (32). Therefore the total load that can be carried by a stiffened curved sheet panel is given by the equation

$$P_{TOT} = \sum \sigma_{st} (A_1 + A_2) + \sum (b - 2w) t \tag{43}$$

where the first term indicates the contribution of the edges of the sheet with the attached stiffener sections and the second term indicates the contribution of the center portion of the sheet, or the part due to the curvature of the panel.

The calculation of the predicted load on the basis of equations (41) and (43) has been made for a number of sheet and stiffener combinations tested at M.I.T. and the results are given in Tables IV and V. Table IV gives the

calculations for flat panels and Table V gives the calculated loads for curved panels.

In Table V it will be noticed that in some cases two values are given for the predicted load. These are discussed in detail in Appendix A and it is only necessary to mention here that the specimens giving these values lie outside of the usual range of aircraft monocoque design, inasmuch as they have a very small radius of curvature coupled with a large sheet thickness. Disregarding these values, the remainder of the tests show good agreement between the experimental values of the load and the load predicted by the method just outlined.

In the case of stiffened panels, there arises another variable which as yet has not been discussed. This is the type of attachment between sheet and stiffener and the spacing of the attachment points. On the basis of some recent, unpublished work at C.I.T. on the relative strength of stiffener and sheet attachment methods (Reference 15) it has been found that spot-welding, if well done, gives the highest failure loads, rivets are from 5-15% lower and bolts will give failure loads which are considerably below the loads carried by the riveted specimens. Also, as would be expected, the failure loads drop off as the spacing of the attachment points is increased.

It will be noticed in Table V that there does not seem to be any consistent variation in the load carried by the panels for different lengths of specimens, other than that expected from a shortening of the column. In other words, the discrepancies between the predicted and actual loads are not a function of the length of the specimen.

One of the most probable sources of error, and a very likely source of experimental scatter, for both the stiffened and unstiffened panels which were tested at M.I.T. lies in the fact that constant values for E and σ_y have been taken throughout, owing to lack of more complete data by the author. The assumption of $E = 10^7$ lbs./sq.in. is probably correct to ± 5%; however, the assumption of $\sigma_y = 36{,}000$ lbs./sq.in. is much more doubtful, since this value varies within comparatively wide limits for different sheets of the same thickness, different directions in the same sheet, and for sheets of different thicknesses. It is expected that the experimental scatter could be appreciably decreased if the actual values of E and σ_y were to be used for each separate panel tested. The values assumed, however, are good mean values, and the use of the true values for each panel would probably not appreciably alter the average correlation between experiment and theory.

Another possible source of scatter for the stiffened panels lies in the testing method used. The panels were made up, the ends were machined parallel and were then tested in a parallel head testing machine as flat ended columns. This tends to give a very doubtful value of the end fixity as the effective end fixity will have a tendency to vary with different thicknesses of sheet, the accuracy of the machining operation, the type of panel tested, etc.

For the above two reasons, i.e. that the actual physical properties of the materials were not available, and that the end fixity of the panels was somewhat doubtful, it appears to the author that the obtained scatter between

experimental and theoretical values is not excessive, and that the method used to calculate the predicted load on stiffened panels is applicable to practical design.

Conclusion

For the case of flat and curved unstiffened panels it is thought that the combination of the assumed theoretical treatment as a special problem in small deflections and the physical analysis of a large number of experimental tests has lead to what are probably the two fundamental equations for sheets under compression, i.e.

$$P = C\sqrt{E\sigma}\,t^2$$

$$C = f(\lambda,\eta) = f\left(\sqrt{\frac{E}{\sigma}}\frac{t}{b}, \sqrt{\frac{E}{\sigma}}\frac{b}{R}\right)$$

and that experimental tests have determined empirical values for C as a function of λ and η which are applicable to design. In order to obtain a theoretical curve which would correspond to that found empirically, it will be necessary to go to a more elaborate analysis of the problem, using the methods of large deflections.

The application of the above analysis to flat and curved stiffened panels by the assumption of an effective width of sheet acting with the stiffener section is justified by the agreement between experimental tests and calculated total loads. To make this analysis complete, however, there should be considered the type and spacing of the attachment between sheet and stiffeners.

Although the tests on curved sheet have all been made on duralumin, it is felt that the method used will apply equally well to other materials. The strength of the supported sides of the panel has been found to be given by the above equations very satisfactorily for any material and the allowable stress in the center section is taken from tests on complete cylinders which have covered quite a large

range of materials.

Appendix A gives in detail the method of calculating a stiffened panel and Appendix B contains the curves of C and C_f as well as several curves which simplify the calculations of values needed in using this method.

References

1--G.H.Bryan--Proc. London Math. Soc. Vol. 22, 1891

2--S.Timoshenko--Strength of Materials, Part II.

3--A.E.H.Love--Mathematical Theory of Elasticity.

4--A.Nadai--Elastiche Platten.

5--A.Foppl--Drang und Zwang.

6--J.S.Newell--Airway Age--Nov. and Dec. 1930

7--L.Schuman and G.Back--N.A.C.A. Report No. 356.

8--Th. von Karman, E.E.Sechler, L.H.Donnell--Applied Mech. Trans. of the A.S.M.E.--June 1932.

9--H.L.Cox--Reports and Memoranda No. 1554.

10--R.W.Mossman and R.G.Robinson--N.A.C.A. Tech. Note No. 357

11--S.C.Redshaw--Reports and Memoranda No. 1565.

12--E.E.Lundquist--N.A.C.A. Report No. 473

13--J.S.Newell and W.H.Gale--A Report on Aircraft Materials Research at the Mass. Inst. of Tech., 1932.

14--E.E.Lundquist--N.A.C.A. Tech. Note No. 455.

15--C.B.Hutchins--The Relative Strength of Stiffener and Sheet attachment Methods. C.I.T. 1934.

Appendix A

Type Calculations for Stiffened Panels.

The method of calculating the ultimate load that can be supported by a stiffened sheet panel is best illustrated by examples. It involves, as mentioned previously, the computation of the effective width of sheet which can be considered to be acting with the stiffener as a column and the failing stress of the combined column, which is a function of the radius of gyration, the length, and the end fixity. The procedure is essentially the same as that proposed by Lundquist (Reference 14).

In order to facilitate calculations, a curve showing the variation of the radius of gyration with width of attached sheet is necessary. By a very ingenious calculation, G. White of C.I.T. arrived at an equation which gives this variation immediately in terms of the known variables for any section. Since the failing stress of a column is directly proportional to the square of the radius of gyration, the equation is written in the form

$$\left(\frac{\rho}{\rho_0}\right)^2 = \frac{\sigma}{\sigma_0} = \frac{1+\left[1+\left(\frac{S}{\rho_0}\right)^2\right]\frac{\ell t}{A_0}}{\left(1+\frac{\ell t}{A_0}\right)^2} \qquad \text{(A-1)}$$

where

ρ_0 = radius of gyration of the stiffener alone

ρ = radius of gyration of the stiffenmr plus the attached sheet.

A_0 = area of stiffener alone

S = distance from the center of the sheet to the neutral axis of the stiffener.

t = thickness of the sheet

ℓ = total width of sheet acting with the stiffener

The above equation has been put into curve form and is given in Fig. B-3.

In the above equation ℓ is taken as the total

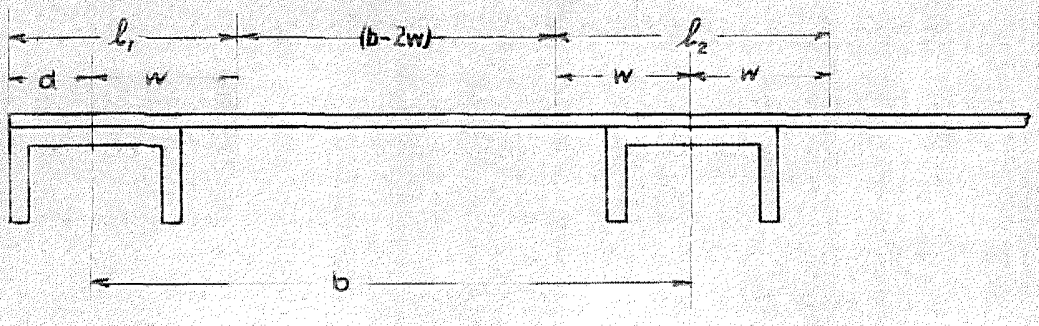

FIG. A-1

width of sheet acting with the stiffener (See Fig. A-1). In the case of a continuous structure the value of ℓ would obviously be twice the effective width, or

$$\ell = 2w$$

In the case of a structure, where there was a sheet panel ending in a stiffener section then

$$\ell = w + d$$

where "d" is calculated as follows:

For the sheet overhang beyond the stiffener attachment point, the sheet is considered bo be acting as a panel simply supported on three sides with the fourth side free. The buckling stress of such a panel is given by an equation which can be put into a form giving the effective width of such a panel for a given stress, as

$$d = .673 \sqrt{\frac{E}{\sigma_{cr}}}\, t \qquad (A\text{-}2)$$

Whenever "d" as found above is less than the actual overhang distance, the calculated value is used; when the above value of "d" is greater than the overhang value, it is obvious that the actual measured distance is used.

Example 1--Consider first the flat sheet panel, No. 11, Table IV. The known values are

$t = .019"$

$A_0 = .0566$ sq. in.

$\rho_0 = .1600"$

$\bar{y} = .156 + t/2 = .1655"$

$b = 5.625"$

$\sigma_0 = 22800$ #/in^2

$E = 9.8 \times 10^6$ #/in^2

From which we can calculate, using either their respective equations or the curves in Appendix B,

$t/A_0 = .3359$ $\qquad \bar{y}/\rho_0 = 1.035$

$\lambda = .0699$

$C_f = 1.82$ (Fig. B-1)

$w = .358"$

$d = .673\sqrt{\frac{E}{\sigma}}\,t = .265"$

$l = w + d = .623"$

$\frac{\sigma}{\sigma_0} = .98$ (Fig. B-3)

$\sigma = 22300$ #/in^2

Repeating the process, using this new value of σ_{st} we get

$\lambda = .0705$

$C_f = 1.82$

$w = .362"$

$d = .268"$

$l = .630$

$\sigma/\sigma_0 = .98$

$\therefore \sigma_{design} = 22300$ #/in^2

and the total area under this stress is

$A = 2 \times .0566 + 2 \times .019 \times .630 = .1372$ in^2

Then the load carried by the two end stiffeners is

$P_e = .1372 \times 22300 = 3060$#

The effective width of sheet acting with the center stiffeners is

$l = 2w = .716"$

and, from Fig. B-8

$$\sigma/\sigma_0 = .97 \qquad \sigma = 22100^{\#}/\square''$$

The second approximation gives

$$\lambda = .0711$$
$$C_f = 1.82$$
$$w = .364''$$
$$\ell = .728''$$
$$\sigma/\sigma_0 = .97$$
$$\therefore \sigma_{design} = 22100^{\#}/\square''$$

The total area under this stress is

$$A = 2 \times .364 \times .019 + .0566 = .0705\ \square''$$

and the load carried by the center stiffener is

$$P_c = .0705 \times 22100 = 1560^{\#}$$

This gives a total load carried by the panel as

$$P_{TOT} = P_e + P_c = 3060 + 1560 = 4620^{\#}$$

For a stiffened curved sheet panel, the procedure is the smae except that there must be added the load carried by the center portion of the sheet of width $(b - 2w)$, which is subjected to the stress σ_c. This load is

$$P_{center} = (b-2w)t\sigma_c$$

which is carried in addition to the load carried by the stiffener plus the attached sheet. This is the method that has been followed in calculating the values of Table V.

In Table V there will be noticed a number of specimens for which two calculated values have been shown. The first value listed is that obtained by the method outlined above, in which the stiffeners take a stress σ_{st_1} and σ_{st_2} respectively, and center of the sheet takes a stress σ. Consider, for example, the 12" long specimen with three stiffeners, made of 0.052" sheet and bent to a radius of 5". In this case

σ_{st_1} = 17700 lbs./sq.in.

σ_{st_2} = 14400 lbs./sq.in.

σ_c = 31200 lbs./sq.in.

Calculated in the ordinary manner, the predicted load is given by

$$P_{TOT} = P_1 + P_2 = 6870 + 12060 = 18930^{\#}$$

which is 13% above the actual load obtained in test.

Since, in the above case, the failing stress of all of the stiffeners is far below the allowable compressive stress of the curved sheet, the stiffeners very likely buckle at their failing stress and precipitate failure of the curved sheet between them, long before the sheet has reached its maximum allowable stress. For this reason, it is suggested that for conservative design for this case, the whole panel be assumed to fail as soon as the stiffener with the highest value of σ_{st} reaches its failing stress, and that the sheet between stiffeners can undergo no higher stresses than this value of $\sigma_{st(max)}$. If this method is used, then in the above example,

$$P_2' = 12060 \times 17700/31200 = 6840^{\#}$$

and the total load carried by the panel is given by

$$P_{TOT} = 6870 + 6840 = 13710^{\#}$$

which is 18% below the value obtained by test.

It is obvious from an inspection of the results in Table V that the higher critical stress values of the sheet tend to retard failure of the stiffeners, but since the amount of this effect is largely unknown it seems preferable to ignore it altogether, and design as indicated above

The above cases correspond to points in Fig. B-2 to the right of the limiting line, and we are assuming that these points can never be reached. (52)

Appendix B

Tables and Curve Sheets

TABLE I

No	MATER.	b"	t"	P#	$E^{\#}/\square'' \times 10^{-7}$	σ_y #/□"	$\sqrt{E\sigma_y}$	C_f	λ
(1)	(2)	(3)	(4)	(5)	(6)	(7)	(8)	(9)	(10)
1	DURAL	12	.0664	4,760	1.023	27,330	5.29×10^5	2.045	.1065
2	"	4	.0660	3,830	1.023	27,330	5.29 "	1.676	.3160
3	"	18	.0666	4,930	1.037	40,400	6.47 "	1.711	.0597
4	"	8	.0671	4,400	1.037	40,400	6.47 "	1.511	.1356
5	"	2	.0672	3,880	1.037	40,400	6.47 "	1.327	.5360
6	"	2	.0671	3,680	1.037	40,400	6.47 "	1.264	.5360
7	STEEL	3½	.0113	140	2.684	24,550	8.13 "	1.349	.1152
8	"	4	.0116	190	2.963	26,160	8.81 "	1.602	.0960
9	"	6	.0115	180	2.684	24,550	8.13 "	1.673	.0630
10	"	12	.0113	200	2.963	26,160	8.81 "	1.779	.0315
11	"	16	.0113	220	2.845	25,300	8.49 "	2.028	.0238
12	"	8	.0111	190	2.690	23,600	7.98 "	1.931	.0469
13	"	4	.0115	170	2.645	24,200	8.00 "	1.615	.0950
14	"	3	.0114	150	2.645	24,200	8.00 "	1.430	.1264
15	"	2	.0113	160	2.645	24,200	8.00 "	1.580	.1860
16	ALUMINUM	4	.0510	1,420	.901	10,250	3.04 "	1.790	.3805
17	"	7	.0499	1,360	.935	9,450	3.01 "	1.854	.2225
18	"	12	.0500	1,575	.901	10,250	3.04 "	2.200	.1237
19	STEEL	8	.0113	190	2.958	28,900	9.25 "	1.595	.0457
20	"	3	.0159	330	2.820	25,000	8.41 "	1.559	.1750
21	"	2½	.0161	290	2.820	25,000	8.41 "	1.340	.2128
22	"	2	.0159	290	2.820	25,000	8.41 "	1.352	.3640
23	"	1½	.0159	295	2.820	25,000	8.41 "	1.360	.3507
24	"	1	.0157	230	2.820	25,000	8.41 "	1.109	.5195
25	"	2	.0518	2,420	2.278	35,900	9.04 "	1.000	.6530
26	"	3	.0520	2,720	2.278	35,900	9.04 "	1.111	.4370
27	"	3	.0513	2,510	2.278	35,900	9.04 "	1.059	.4310
28	DURAL	1½	.0664	2,850	1.037	40,400	6.47 "	.997	.7130
29	"	1	.0667	1,750	1.037	40,400	6.47 "	.608	1.0740
30	"	2	.0670	3,830	1.037	40,400	6.47 "	1.318	.5345
31	"	1½	.0664	3,260	1.037	40,400	6.47 "	1.125	.7140
32	"	1¼	.0663	2,785	1.037	40,400	6.47 "	.979	.8540
33	BRASS	6	.0160	335	1.686	37,000	7.90 "	1.666	.0567
34	"	4	.0158	335	1.686	37,000	7.90 "	1.765	.0841
35	"	3	.0157	365	1.686	37,000	7.90 "	1.820	.0959

$$C_f = \frac{P}{\sqrt{E\sigma_y}\, t^2} \qquad \lambda = \sqrt{\frac{E}{\sigma_y}}\,\frac{t}{b}$$

TABLE No. II

$$\lambda = \sqrt{\frac{E}{\sigma_y}}\,\frac{t}{b} \qquad C_f = \frac{P_{TEST}}{\sqrt{E\sigma_y}\,t^2} \qquad w_e = \frac{C_f}{2}\sqrt{\frac{E}{\sigma_y}}\,t$$

TEST No.	MATER.	LENG. in.	WIDTH in.	L/b	THICK. in.	$E^{\#}/in.^2$ $\times 10^{-6}$	$\sigma_y^{\#}/in.^2$	$\sqrt{\frac{E}{\sigma_y}}\,t$	λ	$P_{TEST}^{\#}$	$\sqrt{E\sigma_y}\,t^2$	C_f	w_e"
401	STEEL	3	.828	3.63	.0263	30.37	34,000	.787	.950	655	703	.93	.362
402	DURAL	"	1.140	2.63	.0651	10.00	35,300	1.045	.962	2135	2519	.85	.465
403	STEEL	"	.995	3.02	.0275	30.37	34,000	.823	.827	670	768	.87	.358
404	DURAL	"	1.400	2.14	.0640	10.00	35,300	1.027	.769	2465	2436	1.01	.540
405	STEEL	"	1.430	2.10	.0264	30.37	34,000	.788	.551	605	706	.86	.334
406	DURAL	"	2.000	1.50	.0641	10.00	35,300	1.078	.539	3890	2443	1.59	.857
407	STEEL	"	2.010	1.49	.0264	30.37	34,000	.788	.393	820	706	1.16	.457
408	DURAL	"	1.735	1.73	.0342	10.00	45,000	.510	.294	1065	786	1.36	.347
409	STEEL	"	1.775	1.69	.0122	26.02	30,000	.359	.203	200	132	1.52	.273
410	DURAL	"	3.500	.86	.0322	10.00	45,000	.480	.137	1015	696	1.46	.350
411	STEEL	"	3.005	1.00	.0125	26.02	30,000	.368	.122	215	138	1.56	.287
412	DURAL	"	4.990	.60	.0334	10.00	45,000	.498	.100	1265	748	1.69	.421
413	STEEL	"	4.990	.60	.0127	26.02	30,000	.374	.075	240	143	1.68	.314
414	DURAL	"	10.030	.30	.0324	10.00	45,000	.483	.048	1660	705	2.35	.568
415	STEEL	"	16.010	.20	.0112	26.02	30,000	.330	.022	280	111	2.52	.416
416	STEEL	6	.840	7.14	.0262	30.37	34,000	.784	.934	725	697	1.02	.407
417	DURAL	"	1.145	5.24	.0637	10.00	35,300	1.072	.937	2945	2410	1.22	.654
418	STEEL	"	1.000	6.00	.0264	30.37	34,000	.789	.789	785	708	1.11	.438
419	DURAL	"	1.410	4.26	.0637	10.00	35,300	1.072	.761	3380	2410	1.40	.750
420	STEEL	"	1.410	4.26	.0263	30.37	34,000	.787	.559	740	703	1.05	.413
421	DURAL	"	2.025	2.96	.0638	10.00	35,300	1.073	.530	3950	2420	1.63	.874
422	STEEL	"	1.990	3.01	.0265	30.37	34,000	.792	.399	795	713	1.14	.443
423	DURAL	"	1.730	3.47	.0340	10.00	45,000	.507	.293	1005	776	1.30	.329
424	STEEL	"	1.760	3.41	.0118	26.02	30,000	.347	.198	190	123	1.54	.267
425	DURAL	"	3.515	1.71	.0320	10.00	45,000	.477	.136	1150	687	1.67	.398
426	STEEL	"	3.035	1.98	.0119	26.02	30,000	.351	.116	150	125	1.20	.210
427	DURAL	"	5.010	1.19	.0318	10.00	45,000	.474	.095	1310	678	1.93	.457
428	STEEL	"	4.990	1.20	.0116	26.02	30,000	.342	.068	210	119	1.76	.301
429	DURAL	"	10.010	.60	.0317	10.00	45,000	.458	.046	1620	674	2.40	.550
430	STEEL	"	15.020	.40	.0118	26.02	30,000	.347	.023	250	123	2.03	.362
431	STEEL	9	.850	10.58	.0266	30.37	34,000	.795	.935	675	716	.94	.373
432	DURAL	"	1.130	7.96	.0642	10.00	35,300	1.081	.956	2670	2445	1.09	.589
433	STEEL	"	.995	9.02	.0268	30.37	34,000	.801	.805	605	718	.84	.336
434	DURAL	"	1.415	6.36	.0643	10.00	35,300	1.082	.766	3440	2445	1.40	.757
435	STEEL	"	1.400	6.43	.0264	30.37	34,000	.788	.563	965	706	1.37	.540
436	DURAL	"	2.005	4.49	.0643	10.00	35,300	1.082	.540	3670	2455	1.44	.779
437	STEEL	"	2.005	4.49	.0280	30.37	34,000	.837	.418	1135	795	1.43	.598
438	DURAL	"	1.725	5.22	.0335	10.00	45,000	.499	.289	1150	753	1.52	.379
439	STEEL	"	1.730	5.20	.0126	26.02	30,000	.371	.215	200	140	1.43	.265
440	DURAL	"	3.515	2.56	.0356	10.00	45,000	.531	.151	1175	850	1.38	.366
441	STEEL	"	3.015	2.98	.0128	26.02	30,000	.377	.125	280	145	1.93	.364
442	DURAL	"	5.015	1.79	.0330	10.00	45,000	.492	.098	1175	730	1.61	.396
443	STEEL	"	5.005	1.80	.0128	26.02	30,000	.377	.075	225	145	1.55	.292
444	DURAL	"	10.000	.90	.0346	10.00	45,000	.516	.052	1220	804	1.52	.392
445	STEEL	"	15.020	.60	.0130	26.02	30,000	.383	.026	245	149	1.65	.316
446	STEEL	12	.825	14.55	.0264	30.37	34,000	.789	.956	655	707	.93	.371
447	DURAL	"	1.125	10.66	.0630	10.00	35,300	1.074	.955	2300	2417	.95	.510
448	STEEL	"	1.015	11.82	.0252	30.37	34,000	.753	.742	780	644	1.21	.456
449	DURAL	"	1.430	8.39	.0629	10.00	35,300	1.075	.752	2690	2350	1.14	.613
450	STEEL	"	1.410	8.51	.0262	30.37	34,000	.783	.555	780	696	1.12	.438
451	DURAL	"	2.015	5.96	.0627	10.00	35,300	1.071	.532	3630	2335	1.55	.831
452	STEEL	"	2.000	6.00	.0266	30.37	34,000	.795	.398	955	716	1.34	.532
453	DURAL	"	1.740	6.90	.0313	10.00	45,000	.467	.268	860	657	1.31	.306
454	STEEL	"	1.745	6.88	.0118	26.02	30,000	.348	.199	205	123	1.67	.291
455	DURAL	"	3.495	3.43	.0332	10.00	45,000	.495	.142	955	739	1.29	.319
456	STEEL	"	3.015	3.98	.0117	26.02	30,000	.345	.114	215	121	1.78	.306
457	DURAL	"	5.010	2.40	.0339	10.00	45,000	.506	.101	1380	772	1.79	.453
458	STEEL	"	4.995	2.41	.0120	26.02	30,000	.353	.071	250	127	1.97	.348
459	DURAL	"	10.030	1.20	.0329	10.00	45,000	.491	.049	1110	728	1.52	.373
460	STEEL	"	15.000	.80	.0118	26.02	30,000	.348	.023	280	123	2.28	.410

TABLE NO. II (con.)

TEST No.	MATER.	LENG. in.	WIDTH in.	L/b	THICK. in.	$E^{\#}/\square''$ x10^{-6}	σ_y $^{\#}/\square''$	$\sqrt{\frac{E}{\sigma_y}}\,t$	λ	P_{test}^{*}	$\sqrt{E\sigma_y}\,t^2$	C_f	We in.
461	STEEL	15	.830	18.07	.0259	30.37	34,000	.774	.933	580	600	.85	.329
462	DURAL	"	1.125	13.34	.0630	10.00	35,300	1.060	.942	2790	2360	1.18	.625
463	STEEL	"	1.010	14.85	.0259	30.37	34,000	.774	.766	650	680	.96	.312
464	DURAL	"	1.395	10.76	.0630	10.00	35,300	1.060	.780	2730	2360	1.16	.615
465	STEEL	"	1.420	10.56	.0258	30.37	34,000	.771	.543	745	675	1.10	.424
466	DURAL	"	1.925	7.79	.0632	10.00	35,300	1.063	.552	3770	2375	1.59	.846
467	STEEL	"	1.980	7.58	.0262	30.37	34,000	.782	.395	840	695	1.21	.414
468	DURAL	"	1.315	8.15	.0334	10.00	45,000	.498	.290	880	750	1.17	.291
469	STEEL	"	1.745	8.59	.0120	26.02	30,000	.353	.203	200	127	1.58	.279
470	DURAL	"	3.490	4.30	.0330	10.00	45,000	.492	.141	1095	732	1.50	.369
471	STEEL	"	3.005	5.00	.0118	26.02	30,000	.348	.116	240	123	1.72	.299
472	DURAL	"	5.010	2.99	.0335	10.00	45,000	.500	.100	1095	754	1.46	.365
473	STEEL	"	5.005	3.00	.0120	26.02	30,000	.353	.071	225	127	1.77	.213
474	DURAL	"	10.010	1.50	.0335	10.00	45,000	.500	.050	1240	754	1.64	.410
475	STEEL	"	15.020	1.00	.0118	26.02	30,000	.348	.023	265	123	2.16	.316
476	STEEL	18	.800	22.50	.0260	30.37	34,000	.777	.972	500	685	.73	.284
477	DURAL	"	1.130	15.93	.0632	10.00	35,300	1.063	.941	2895	2315	1.22	.648
478	STEEL	"	1.000	18.00	.0266	30.37	34,000	.795	.795	745	718	1.04	.413
479	DURAL	"	1.410	12.76	.0630	10.00	35,300	1.060	.752	2870	2360	1.22	.647
480	STEEL	"	1.420	12.67	.0254	30.37	34,000	.760	.535	645	655	.99	.316
481	DURAL	"	2.010	8.96	.0625	10.00	35,300	1.051	.523	2590	2320	1.12	.588
482	STEEL	"	2.010	8.96	.0260	30.37	34,000	.777	.386	870	685	1.27	.493
483	DURAL	"	1.110	10.53	.0331	10.00	45,000	.494	.289	800	735	1.09	.409
484	STEEL	"	1.758	10.24	.0116	26.02	30,000	.342	.194	200	119	1.68	.287
485	DURAL	"	3.520	5.12	.0332	10.00	38,500	.519	.148	845	643	1.31	.340
486	STEEL	"	3.000	6.00	.0118	26.02	30,000	.348	.116	180	123	1.47	.255
487	DURAL	"	5.020	3.59	.0327	10.00	38,500	.521	.105	1010	662	1.53	.403
488	STEEL	"	5.000	3.60	.0118	26.02	30,000	.348	.070	200	123	1.63	.283
489	DURAL	"	10.030	1.79	.0338	10.00	45,000	.504	.050	1180	765	1.54	.388
490	STEEL	"	14.980	1.20	.0118	26.02	30,000	.348	.023	225	123	1.83	.318
491	STEEL	21	.813	25.82	.0260	30.37	34,000	.777	.955	545	685	.80	.311
492	DURAL	"	1.140	18.42	.0625	10.00	35,300	1.051	.922	2915	2320	1.26	.662
493	STEEL	"	1.010	20.79	.0260	30.37	34,000	.777	.769	645	685	.94	.360
494	DURAL	"	1.390	15.10	.0625	10.00	35,300	1.051	.756	3295	2320	1.42	.746
495	STEEL	"	1.410	14.90	.0258	30.37	34,000	.771	.547	1005	675	1.49	.574
496	DURAL	"	2.000	10.50	.0625	10.00	35,300	1.051	.526	3520	2320	1.52	.799
497	STEEL	"	2.010	10.45	.0262	30.37	34,000	.781	.389	740	696	1.06	.415
498	DURAL	"	1.720	12.21	.0340	10.00	45,000	.507	.295	845	775	1.09	.476
499	STEEL	"	1.770	11.87	.0118	26.02	30,000	.348	.199	200	123	1.63	.283
500	DURAL	"	3.510	5.98	.0338	10.00	45,000	.504	.144	970	766	1.27	.520
501	STEEL	"	3.000	7.00	.0119	26.02	30,000	.351	.111	200	125	1.60	.280
502	DURAL	"	4.990	4.21	.0333	10.00	45,000	.496	.100	865	745	1.16	.388
503	STEEL	"	5.000	4.20	.0120	26.02	30,000	.353	.071	245	127	1.93	.341
504	DURAL	"	10.010	2.10	.0322	10.00	46,000	.480	.048	1230	695	1.83	.439
505	STEEL	"	15.020	1.40	.0123	26.02	30,000	.362	.024	225	134	1.69	.254
506	STEEL	3	10.010	.30	.0264	30.37	34,000	.789	.079	1405	706	1.99	.785
507	DURAL	"	15.010	.20	.0338	10.00	45,000	.504	.034	1940	766	2.53	.638
508	STEEL	"	10.010	.30	.0126	26.02	30,000	.371	.037	270	140	1.93	.358
509	STEEL	"	5.010	.60	.0265	30.37	34,000	.793	.158	945	713	1.33	.526
510	STEEL	"	15.020	.20	.0261	30.37	34,000	.781	.052	1565	691	2.27	.886
511	STEEL	6	15.020	.40	.0270	30.37	34,000	.807	.054	1425	740	1.93	.718
512	DURAL	"	15.010	.40	.0336	10.00	45,000	.501	.033	1570	756	2.05	.514
513	DURAL	12	15.040	.80	.0338	10.00	45,000	.504	.034	1760	766	2.30	.580
514	STEEL	"	15.030	.80	.0269	30.37	34,000	.804	.053	1310	734	1.78	.716
515	DURAL	6	4.00	1.50	.0641	10.00	41,300	.998	.249	3800	2645	1.44	.718
516	DURAL	"	5.75	1.04	.0641	10.00	41,300	.998	.174	4170	2645	1.58	.788

TABLE III

$P_{exp.}$ #	L"	t"	b"	R"	λ	η	C_f	$C_{theor.}$	$C_{exp.}$
950	6	.0200	12	30	.0269	6.67	2.18	4.06	3.96
800	12	"	"	"	"	"	"	"	3.33
620	18	"	"	"	"	"	"	"	2.58
1145	6	"	"	20	"	10.00	"	5.00	4.77
1000	12	"	"	"	"	"	"	"	4.17
735	18	"	"	"	"	"	"	"	3.06
1910	6	"	"	10	"	20.00	"	7.83	7.96
1850	12	"	"	"	"	"	"	"	7.72
1485	18	"	"	"	"	"	"	"	6.19
3200	6	"	"	5	"	40.00	"	13.18	13.33
2600	12	"	"	"	"	"	"	"	10.73
2330	18	"	"	"	"	"	"	"	9.71
825	6	"	9	30	.0371	5.00	2.05	3.44	3.44
685	12	"	"	"	"	"	"	"	2.85
580	18	.0210	"	"	.0389	"	2.00	3.38	2.19
980	6	.0200	"	20	.0371	7.50	2.05	4.13	4.08
850	12	"	"	"	"	"	"	"	3.54
650	18	"	"	"	"	"	"	"	2.71
1620	6	"	"	10	"	15.00	"	6.20	6.76
1310	12	"	"	"	"	"	"	"	5.46
1135	18	"	"	"	"	"	"	"	4.73
2060	6	"	"	5	"	30.00	"	10.37	8.57
2250	12	.0210	"	"	.0389	"	2.00	10.30	8.52
1850	18	.0200	"	"	.0371	"	2.05	10.37	7.70
675	6	"	6	30	.0554	3.33	1.88	2.78	2.81
550	12	"	"	"	"	"	"	"	2.29
555	18	.0210	"	"	.0583	"	1.86	2.75	2.10
755	6	.0200	"	20	.0554	5.00	1.88	3.22	3.14
625	12	"	"	"	"	"	"	"	2.61
575	18	"	"	"	"	"	"	"	2.40
1300	6	"	"	10	"	10.00	"	4.57	5.42
960	12	"	"	"	"	"	"	"	4.00
845	18	"	"	"	"	"	"	"	3.52
1900	6	"	"	5	"	20.00	"	7.26	7.92
1730	12	.0210	"	"	.0583	"	1.86	7.21	6.52
1390	18	.0200	"	"	.0554	"	1.88	7.26	5.80
540	6	"	3	30	.1110	1.67	1.67	2.08	2.25
490	12	"	"	"	"	"	"	2.08	2.04
420	18	.0210	"	"	.1166	"	1.66	2.07	1.59
570	6	.0200	"	20	.1110	2.50	1.67	2.28	2.38
540	12	"	"	"	"	"	"	"	2.25
440	18	"	"	"	"	"	"	"	1.83
795	6	.0210	"	10	.1166	5.00	1.66	2.87	3.01
650	12	.0200	"	"	.1110	"	1.67	2.89	2.71
525	18	"	"	"	"	"	"	"	2.19
1140	6	"	"	5	"	10.00	"	4.11	4.75
960	12	"	"	"	"	"	"	"	4.00
740	18	"	"	"	"	"	"	"	3.08

$E = 10^7$ lbs/sq.in. $\quad \sigma_y = 36{,}000$ lbs/sq.in.

$$\lambda = \sqrt{\frac{E}{\sigma_y}}\,\frac{t}{b} \qquad \eta = \sqrt{\frac{E}{\sigma_y}}\,\frac{b}{R}$$

$$C_{theor.} = (C_f - .3C_f\lambda\eta + .3\eta) \qquad C_{exp.} = \frac{P_{exp}}{\sqrt{E\sigma_y}\,t^2}$$

TABLE III (con.)

P_{exp} #	L"	t"	b"	R"	λ	η	C_f	$C_{theor.}$	$C_{exp.}$
2590	6	.0330	12	30	.0459	6.67	1.94	3.76	3.97
2100	12	"	"	"	"	"	"	"	3.21
1980	18	"	"	"	"	"	"	"	3.03
2635	6	"	"	20	"	10.00	"	4.67	5.57
3370	12	.0335	"	"	.0466	"	"	"	5.00
2760	18	.0330	"	"	.0459	"	"	"	4.22
6580	6	"	"	10	"	20.00	"	7.41	10.06
6085	12	"	"	"	"	"	"	"	9.31
5325	18	"	"	"	"	"	"	"	8.15
9560	6	"	"	5	"	40.00	"	12.87	14.62
9020	12	.0340	"	"	.0472	"	1.93	12.84	13.00
8570	18	.0330	"	"	.0459	"	1.94	12.87	13.11
2250	6	"	9	30	.0612	5.00	1.84	3.19	3.44
1840	12	"	"	"	"	"	"	"	2.82
1725	18	.0340	"	"	.0630	"	1.83	3.16	2.48
3065	6	.0335	"	20	.0621	7.50	"	3.82	4.55
2700	12	.0340	"	"	.0630	"	"	"	3.89
2275	18	.0335	"	"	.0621	"	"	"	3.38
5100	6	"	"	10	"	15.00	"	5.82	7.58
4575	12	.0330	"	"	.0612	"	1.84	5.83	7.00
4030	18	.0335	"	"	.0621	"	1.83	5.82	5.48
7560	6	"	"	5	"	30.00	"	9.81	11.22
6830	12	.0340	"	"	.0630	"	"	9.79	9.73
7010	18	.0330	"	"	.0612	"	1.84	9.83	10.13
1780	6	"	6	30	.0916	3.33	1.72	2.56	2.72
1400	12	"	"	"	"	"	"	"	2.14
1405	18	"	"	"	"	"	"	"	2.15
2240	6	"	"	20	"	5.00	"	2.98	3.43
1995	12	"	"	"	"	"	"	"	3.05
1680	18	.0335	"	"	.0930	"	"	"	2.49
3410	6	.0330	"	10	.0916	10.00	"	4.24	5.22
2790	12	"	"	"	"	"	"	"	4.27
2680	18	.0335	"	"	.0930	"	"	"	3.98
5500	6	"	"	5	"	20.00	"	6.76	8.17
4060	12	.0340	"	"	.0945	"	"	6.75	7.00
4568	18	.0335	"	"	.0930	"	"	6.76	6.78
1210	6	.0330	3	30	.1832	1.67	1.52	1.88	1.85
1110	12	"	"	"	"	"	"	"	1.70
1040	18	.0340	"	"	.1888	"	1.51	1.87	1.50
1420	6	.0330	"	20	.1832	2.50	1.52	2.02	2.17
1300	12	"	"	"	"	"	"	"	1.99
1180	18	.0340	"	"	.1888	"	1.51	2.01	1.70
1905	6	.0330	"	10	.1832	5.00	1.52	2.80	2.92
1725	12	.0340	"	"	.1888	"	1.51	2.78	2.49
1355	18	.0330	"	"	.1832	"	1.52	2.80	2.07
2960	6	.0340	"	5	.1888	10.00	1.51	3.65	4.27
2586	12	"	"	"	"	"	"	"	3.73
2125	18	.0330	"	"	.1832	"	1.52	3.69	3.25

TABLE III (con.)

$P_{exp.}$ #	L"	t"	b"	R"	λ	η	C_f	$C_{theor.}$	$C_{exp.}$
6750	6	.0520	12	30	.0722	6.67	1.79	3.53	4.16
5925	12	.0510	"	"	.0708	"	"	3.54	3.80
5045	18	.0515	"	"	.0715	"	"	3.53	3.17
9060	6	.0520	"	20	.0722	10.00	"	4.40	5.58
8000	12	"	"	"	"	"	"	"	4.93
6815	18	.0515	"	"	.0715	"	"	4.41	4.29
14900	6	.0520	"	10	.0722	20.00	"	7.01	9.18
12310	12	.0510	"	"	.0708	"	"	7.03	7.89
13265	18	.0515	"	"	.0715	"	"	7.02	8.35
19950	6	.0520	"	5	.0722	40.00	"	12.24	12.29
19150	12	.0510	"	"	.0708	"	"	12.27	12.26
19300	18	.0515	"	"	.0715	"	"	12.26	12.14
5220	6	.0500	9	30	.0926	5.00	1.72	2.98	3.48
4500	12	.0510	"	"	.0945	"	"	"	2.88
4205	18	"	"	"	"	"	"	"	2.70
7020	6	.0500	"	20	.0926	7.50	"	3.61	4.68
6150	12	.0510	"	"	.0945	"	"	3.60	3.94
5440	18	"	"	"	"	"	"	"	3.49
11010	6	.0500	"	10	.0926	15.00	"	5.50	7.34
10470	12	"	"	"	"	"	"	"	6.98
9450	18	.0510	"	"	.0945	"	"	5.49	6.06
14500	6	.0500	"	5	.0926	30.00	"	9.29	9.67
13100	12	.0510	"	"	.0945	"	"	9.26	8.40
13425	18	"	"	"	"	"	"	"	8.60
4080	6	.0500	6	30	.1389	3.33	1.60	2.38	2.72
3420	12	"	"	"	"	"	"	"	2.28
3245	18	.0510	"	"	.1416	"	"	2.37	2.08
5365	6	"	"	20	"	5.00	"	2.76	3.44
4500	12	"	"	"	"	"	"	"	2.88
4155	18	"	"	"	"	"	"	"	2.66
7690	6	.0500	"	10	.1389	10.00	"	3.93	5.13
7100	12	"	"	"	"	"	"	"	4.73
6380	18	.0510	"	"	.1416	"	"	3.92	4.09
9900	6	.0500	"	5	.1389	20.00	"	6.27	6.60
9700	12	.0510	"	"	.1416	"	"	6.24	6.22
9000	18	"	"	"	"	"	"	"	5.77
2550	6	"	3	30	.2833	1.67	1.37	1.68	1.63
2160	12	.0500	"	"	.2778	"	"	"	1.44
2050	18	.0510	"	"	.2833	"	"	"	1.31
3135	6	.0500	"	20	.2778	2.50	"	1.83	2.09
2765	12	"	"	"	"	"	"	"	1.85
2255	18	.0510	"	"	.2833	"	"	"	1.44
5000	6	"	"	10	"	5.00	"	2.29	3.20
3820	12	"	"	"	"	"	"	"	2.45
2900	18	"	"	"	"	"	"	"	1.86
5065	6	"	"	5	"	10.00	"	3.21	3.25
5010	12	"	"	"	"	"	"	"	3.21
4190	18	.0500	"	"	.2778	"	"	3.23	2.79

TABLE IV

Stiffener is .75" x .50" x .035" channel $A_o = 0.0506$ sq. in. $\rho_o = .1600$"

Subscripts (1) correspond to end stiffeners; (2) to center stiffeners

σ_o = 27,200 for L=6", 22,800 for L=12", and 15,400 for L=18"

TEST No.	L"	b"	t"	n	σ_{st_1} *"/"	σ_{st_2} *"/"	A_{st_1} "	A_{st_2} "	P_{st_1} *	P_{st_2} *	$P_{calc.}$ *	$P_{exp.}$ *
1	6	11.25	.019	2	26900	—	.1364	—	3610	—	3610	3300
2	"	5.625	"	3	26900	26600	.1334	.0699	3640	1860	5500	5300
3	"	3.75	"	4	26900	26900	.1342	.1368	3610	3680	7290	7100
4	"	11.25	.033	2	25000	—	.1782	—	4460	—	4460	4400
5	"	5.625	"	3	25000	24580	.1144	.0935	4360	2290	6650	7020
6	"	3.75	"	4	25300	24750	.1708	.1194	4310	4440	8760	9500
7	"	11.25	.052	2	20950	—	.2558	—	5360	—	5360	6950
8	"	5.625	"	3	21750	19300	.2368	.1456	5150	2810	7960	11150
9	"	3.75	"	4	22300	19850	.2280	.2710	5090	5380	10470	15000
10	12	11.25	.019	2	22300	—	.1390	—	3100	—	3100	2960
11	"	5.625	"	3	22300	22100	.1372	.0705	3060	1560	4620	4500
12	"	3.75	"	4	22600	22300	.1360	.1398	3015	3120	6195	6470
13	"	11.25	.033	2	20750	—	.1834	—	3810	—	3810	4190
14	"	5.625	"	3	21000	20100	.1768	.0963	3710	1940	5650	6100
15	"	3.75	"	4	21200	20150	.1726	.1830	3660	3800	7460	8450
16	"	11.25	.052	2	17300	—	.2640	—	4570	—	4570	5320
17	"	5.625	"	3	18000	15750	.2430	.1523	4370	2400	6770	9720
18	"	3.75	"	4	18700	16650	.2336	.2832	4370	4720	9090	13200
19	18	11.25	.019	2	15000	—	.1440	—	2160	—	2160	2375
20	"	5.625	"	3	15100	14900	.1318	.0137	2088	1100	3180	3215
21	"	3.75	"	4	15100	15100	.1404	.1426	2120	2160	4280	4450
22	"	11.25	.033	2	13550	—	.1918	—	2600	—	2600	2450
23	"	5.625	"	3	14000	12950	.1930	.1032	2560	1340	3900	4065
24	"	3.75	"	4	14150	13400	.1780	.1952	2520	2620	5140	5600
25	"	11.25	.052	2	11150	—	.2840	—	3170	—	3170	3135
26	"	5.625	"	3	12000	9550	.2598	.1722	3120	1640	4760	4770
27	"	3.75	"	4	12150	9960	.2598	.3264	3160	3220	6380	6620

TABLE V.

R = 80 inches

L"	b"	t"	R/t	n	σ_1 ‰"	σ_2 ‰"	σ_c ‰"	P_{st} #	P_c #	P_{tot} #	P_{exp} #
6	11.25	.0195	4103	2	26700	—	132	3700	150	3850	3450
"	5.625	.0190	4210	3	26800	26800	713	5420	140	5560	5470
"	3.75	"	"	4	26900	26900	"	7250	130	7380	7280
12	11.25	.0195	4103	2	22900	—	132	3140	150	3290	2630
"	5.625	"	"	3	"	22900	"	4640	140	4780	4340
"	3.75	.0190	4210	4	"	"	713	6120	130	6250	6190
18	11.25	"	"	2	15000	—	"	2160	140	2300	2100
"	5.625	.0195	4103	3	15100	15000	132	3240	130	3370	3050
"	3.75	.0190	4210	4	"	"	713	4280	120	4400	4210
6	11.25	.0325	2461	2	25000	—	1219	4340	400	4740	4740
"	5.625	.0320	2500	3	25200	24600	1200	6440	350	6790	6600
"	3.75	.0325	2461	4	"	"	1219	8150	420	8570	9180
12	11.25	.0320	2500	2	20600	—	1200	3670	380	4050	3500
"	5.625	.0335	2388	3	20800	20100	1256	5700	370	6070	5100
"	3.75	"	"	4	21000	20200	"	7600	330	7930	7840
18	11.25	.0330	2425	2	13800	—	1238	2630	400	3030	2530
"	5.625	"	"	3	"	13100	"	3900	340	4240	4100
"	3.75	.0335	2388	4	13850	13000	1256	5190	290	5480	5890
6	11.25	.0515	1553	2	21200	—	1932	5300	930	6230	7150
"	5.625	.0520	1538	3	21100	18600	1950	8070	780	8850	11130
"	3.75	.0515	1553	4	"	18500	1932	10860	580	11440	14960
12	11.25	.0520	1538	2	17500	—	1950	4500	930	5430	4980
"	5.625	"	"	3	17700	14400	"	6870	750	7620	8900
"	3.75	"	"	4	17800	14000	"	9100	520	9620	12630
18	11.25	"	"	2	11000	—	"	3080	890	3970	2710
"	5.625	.0515	1553	3	"	8500	1932	4710	610	5320	4420
"	3.75	.0520	1538	4	12600	10100	1950	6160	560	6720	6310

R = 30 inches

6	11.25	.0190	1579	2	26900	—	1900	3660	380	4040	3750
"	5.625	.0190	"	3	26800	26800	"	5420	360	5780	5700
"	3.75	"	"	4	26900	26900	"	7250	340	7590	7520
12	11.25	.0195	1538	2	22500	—	1950	3140	400	3540	3350
"	5.625	"	"	3	22900	22900	"	4640	380	5020	5190
"	3.75	.0190	1579	4	"	"	1900	6120	340	6460	6560
18	11.25	.0180	1667	2	15150	—	1800	2140	330	2470	2610
"	5.625	"	"	3	15050	15050	"	3140	320	3460	3760
"	3.75	.0190	1579	4	15100	15100	1900	4280	330	4610	4870
6	11.25	.0320	938	2	24900	—	3200	4390	1030	5420	5110
"	5.625	.0325	923	3	25000	24500	3250	6500	970	7470	7650
"	3.75	.0330	909	4	25200	24600	3300	8840	800	9640	10320
12	11.25	.0335	895	2	20450	—	3350	3770	1110	4880	4300
"	5.625	.0320	938	3	20800	20100	3200	5450	920	6370	5700
"	3.75	"	"	4	21100	20300	"	7400	810	8210	8800
18	11.25	.0330	909	2	13810	—	3300	2640	1050	3690	3040
"	5.625	.0325	923	3	13800	13100	3250	3860	890	4750	4950
"	3.75	"	"	4	13950	"	"	4590	750	5340	8000
6	11.25	.0520	577	2	21150	—	5200	5320	2520	7840	8840
"	5.625	"	"	3	21700	18600	"	8070	2080	10150	12200
"	3.75	.0510	588	4	21900	18500	5100	10770	1540	12310	15990
12	11.25	"	"	2	17000	—	"	4400	2390	6790	6150
"	5.625	.0520	577	3	17300	14400	5200	6870	2010	8880	10150
"	3.75	.0515	582	4	17800	14050	5150	9040	1380	10420	14010
18	11.25	.0520	577	2	11000	—	5200	3090	2380	5470	3690
"	5.625	"	"	3	11200	8500	"	4790	1670	6460	5520
"	3.75	"	"	4	11650	9100	"	6390	1100	7490	8350

σ_1 = Failing stress of edge columns

σ_2 = Failing stress of center columns

P_{st} = Total load carried by stiffeners plus attached sheet

P_c = Total load due to curvature.

TABLE V (con.)

R = 10 inches

L"	b"	t"	R/t	n	σ_f #/a"	σ_i #/a"	σ_c #/a"	P_{st} #	P_c #	P_{TOT} #	P_{EXP} #
6	11.25	.0190	526	2	26700	—	5900	3660	1140	4800	3970
"	5.625	"	"	3	26800	26800	"	5420	1090	6510	5950
"	3.75	"	"	4	26900	26900	"	7250	1030	8280	7930
12	11.25	"	"	2	22400	—	"	3110	1130	4240	3600
"	5.625	"	"	3	"	22400	"	4600	1080	5680	5720
"	3.75	"	"	4	"	"	"	6120	1010	1130	7720
18	11.25	"	"	2	15040	—	"	2110	1110	3280	3020
"	5.625	.0195	513	3	15050	15050	5850	3200	1040	4240	4240
"	3.75	.0190	526	4	15100	15100	5900	4280	980	5260	5200
6	11.25	.0330	303	2	24900	—	9900	4460	3230	7690	7450
"	5.625	"	"	3	25000	24500	"	6550	2990	9530	9740
"	3.75	"	"	4	25200	24600	"	8940	2410	10250	11240
12	11.25	.0335	298	2	20450	—	10050	3170	3320	1090	5420
"	5.625	.0320	312	3	20800	20100	9600	5450	2760	8210	7400
"	3.75	"	"	4	21100	20300	"	7400	2430	9830	11100
18	11.25	.0330	303	2	13800	—	9900	2640	3160	5800	3810
"	5.625	"	"	3	"	13100	"	3900	2740	6640	5450
"	3.75	"	"	4	13950	"	"	5280	2290	7570	8450
6	11.25	.0520	192	2	21150	—	15600	5320	7570	12890	15550
"	5.625	.0515	194	3	21200	18500	16050	9060	6380	14440	17600
"	3.75	"	"	4	"	"	15450	10860	4660	15520	19700
12	11.25	.0520	192	2	17500	—	15600	4720	7450	12170	10660
"	5.625	"	"	3	17700	14400	"	6870	6030	12900	13050
"	3.75	"	"	4	17800	14000	"	9100	4180	13280	15700
18	11.25	"	"	2	11000	—	"	3090 3060	7130 5030	10220 8090	4450
"	5.625	"	"	3	11200	8500	"	4740 4160	5020 3600	9810 8340	7550
"	3.75	"	"	4	11250	9100	"	6340 6390	3310 2350	9700 8770	10520

R = 5 inches

6	11.25	.0190	263	2	26700	—	11400	3660	2270	5930	4750
"	5.625	"	"	3	26800	26800	"	5420	2170	7590	6830
"	3.75	"	"	4	26900	26900	"	7250	2050	9300	9100
12	11.25	"	"	2	22400	—	"	3110	2260	5370	3970
"	5.625	"	"	3	"	22400	"	4600	2150	6750	6340
"	3.75	"	"	4	"	"	"	6120	2020	8140	8880
18	11.25	.0195	256	2	15000	—	11700	2190	2340	4530	4170
"	5.625	.0190	263	3	"	15000	11400	3200	2090	5290	5590
"	3.75	.0195	256	4	"	"	[illegible]	4300	2030	6330	7390
6	11.25	.0330	151	2	24900	—	19800	4460	6410	10870	8200
"	5.625	"	"	3	25000	24500	"	6550	5970	12520	10230
"	3.75	.0335	149	4	"	"	20100	8860	5420	14180	13000
12	11.25	"	"	2	20450	—	"	3170	6640	10460	10100
"	5.625	"	"	3	20800	20100	"	5700	5790	11690	10500
"	3.75	.0320	156	4	21100	20300	19200	7400	4850	12250	12600
18	11.25	.0330	151	2	13800	—	19800	2640	6320 4430	8960 1010	5530
"	5.625	"	"	3	"	13100	"	3900	5480 3820	9380 7720	9520
"	3.75	"	"	4	13950	"	"	5280	4570 3220	9850 8500	11930
6	11.25	.0520	96	2	21150	—	31200	5320	15150 10510	20470 15830	19080
"	5.625	"	"	3	21700	18600	"	8070	12490 8640	20560 16160	21500
"	3.75	"	"	4	"	18400	"	10920	9400 6530	20320 17450	24300
12	11.25	"	"	2	17500	—	"	4720	14900 8360	19620 13080	14300
"	5.625	"	"	3	17700	14400	"	6870	12060 6840	18930 13310	16700
"	3.75	"	"	4	17800	14000	"	9100	8360 4765	17460 13860	19800
18	11.25	"	"	2	11000	—	"	3090	14250 5030	17340 8120	10300
"	5.625	"	"	3	11200	8500	"	4740	10010 3600	14500 8340	13730
"	3.75	"	"	4	11250	9100	"	6340	6610 2350	13000 8770	16090

Curve for The Determination of C_f

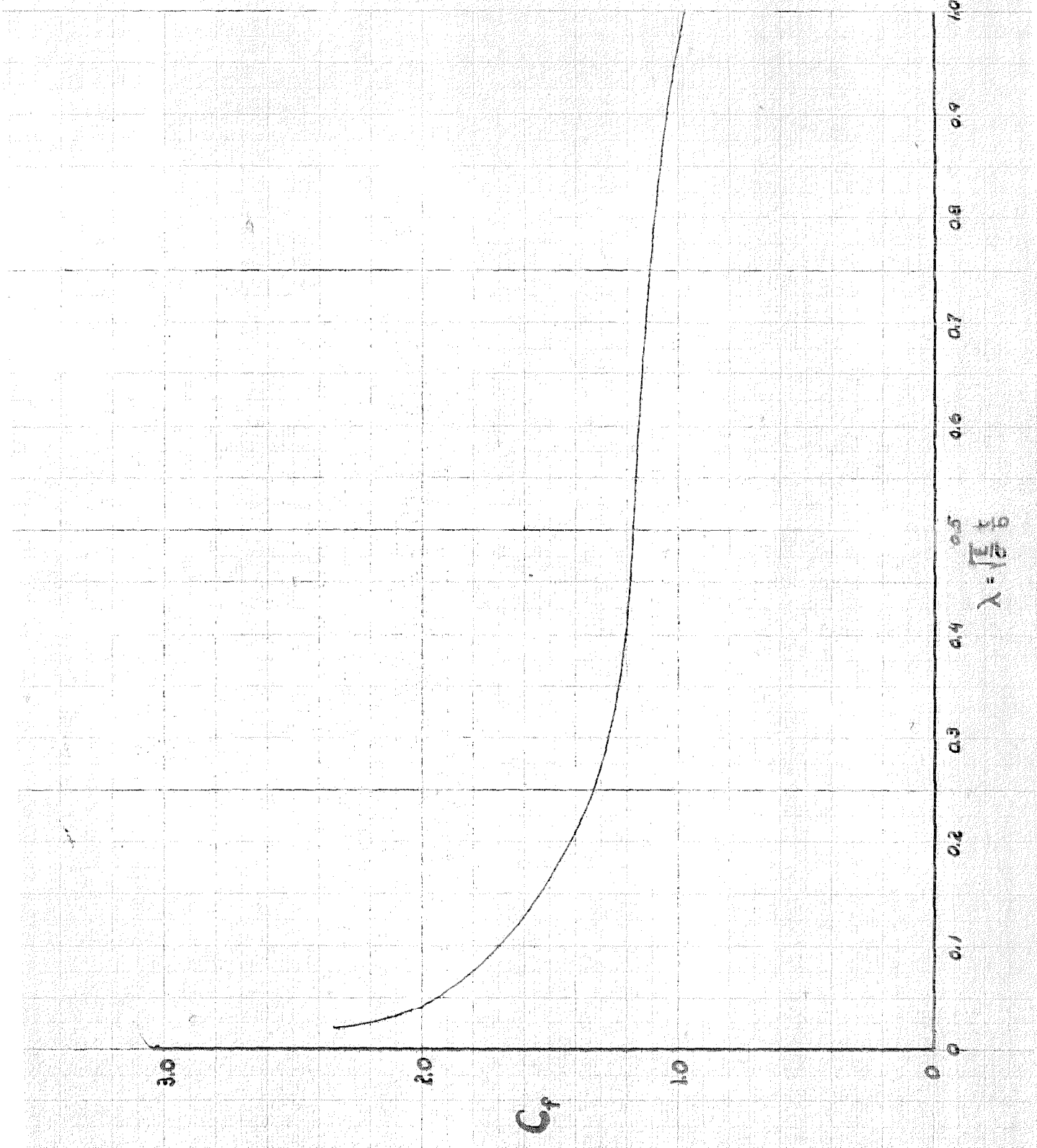

Fig. B-1

CURVE FOR THE DETERMINATION OF $\sqrt{\frac{E}{q}}t$ AND $\lambda = \sqrt{\frac{E}{q}}\frac{t}{D}$

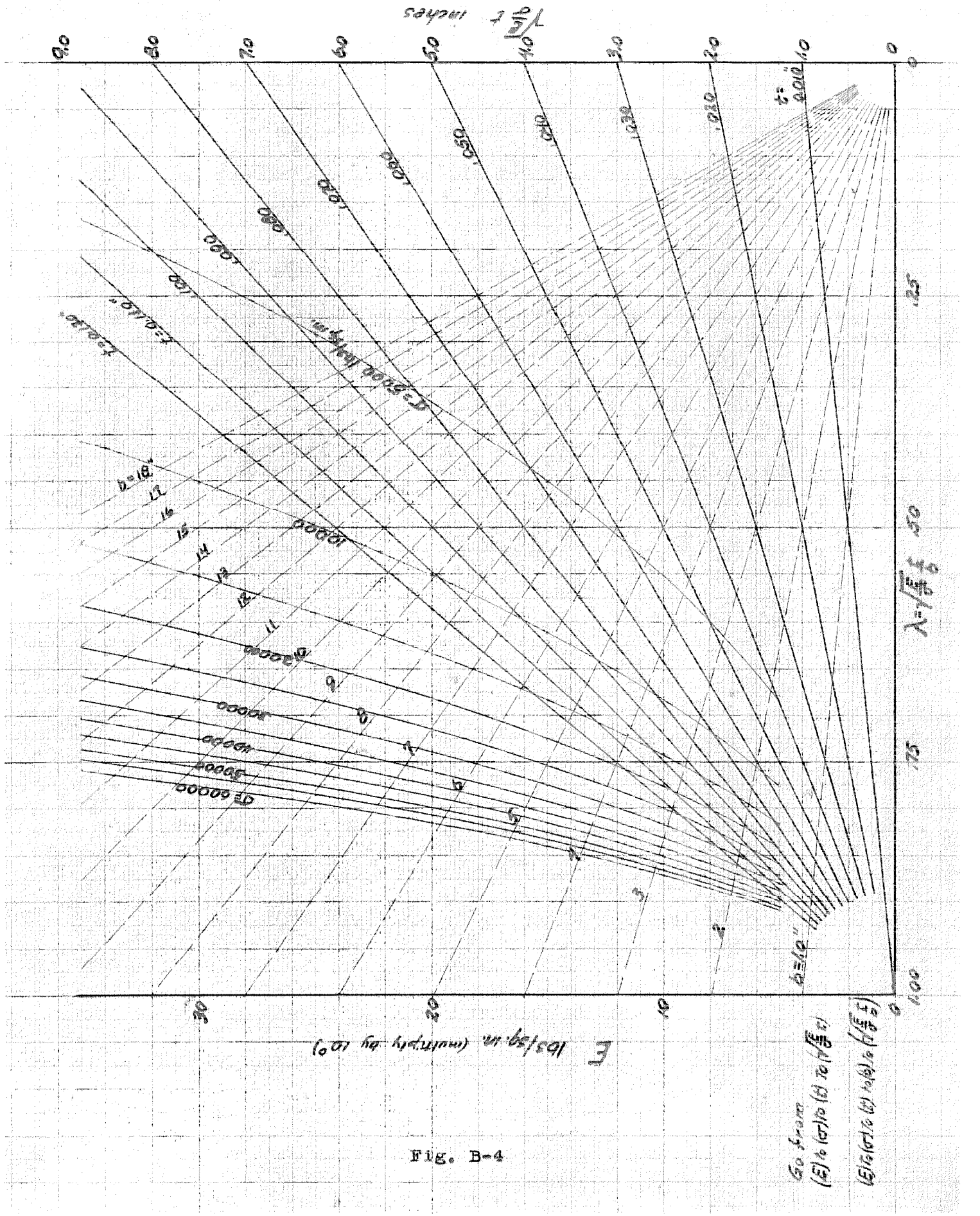

Fig. B-4

Curve for the Determination of $\sqrt{E\sigma}\, t^2$

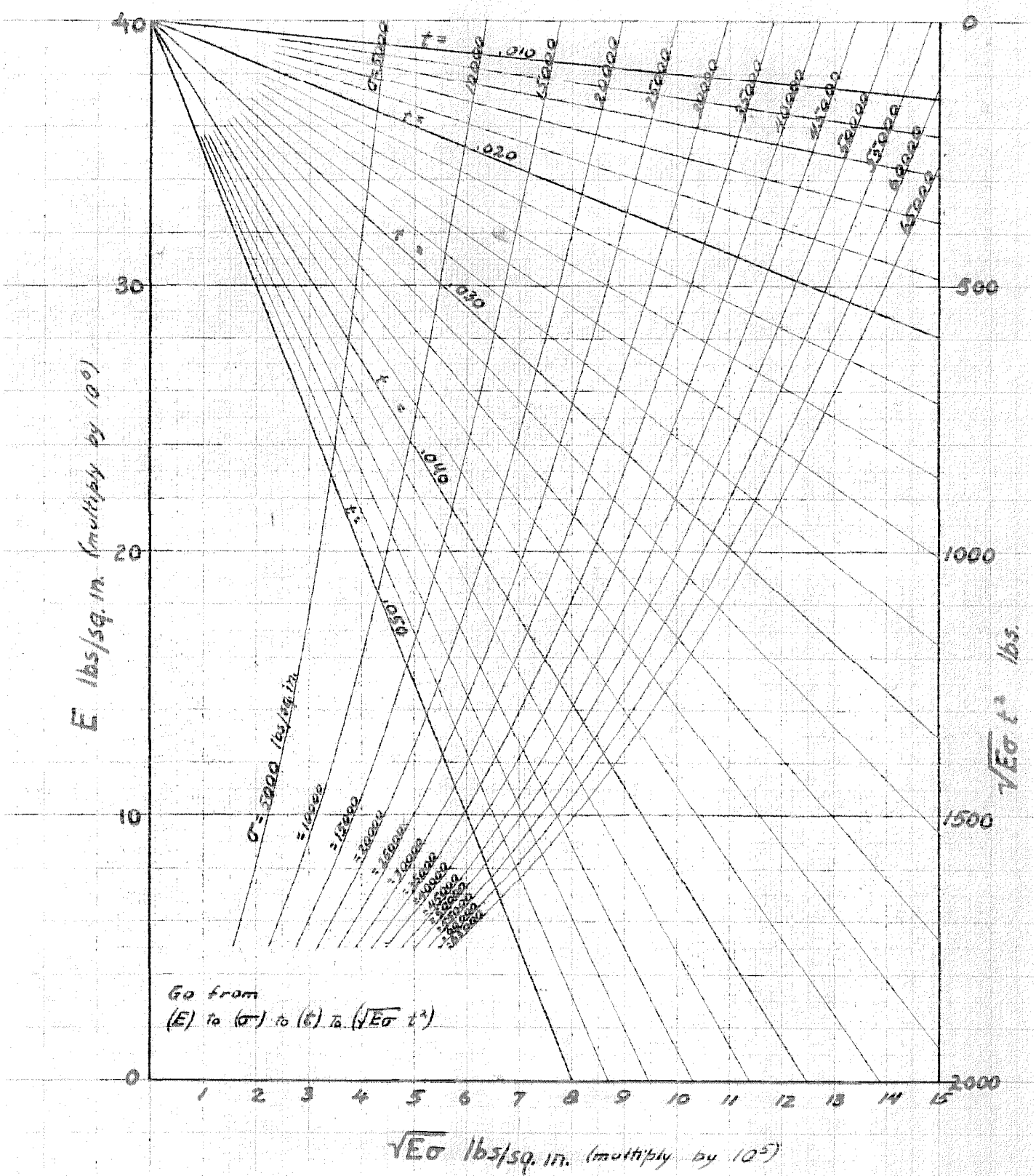

Fig. B-5

Curve for the Determination of $\sqrt{E\sigma}\, t^2$

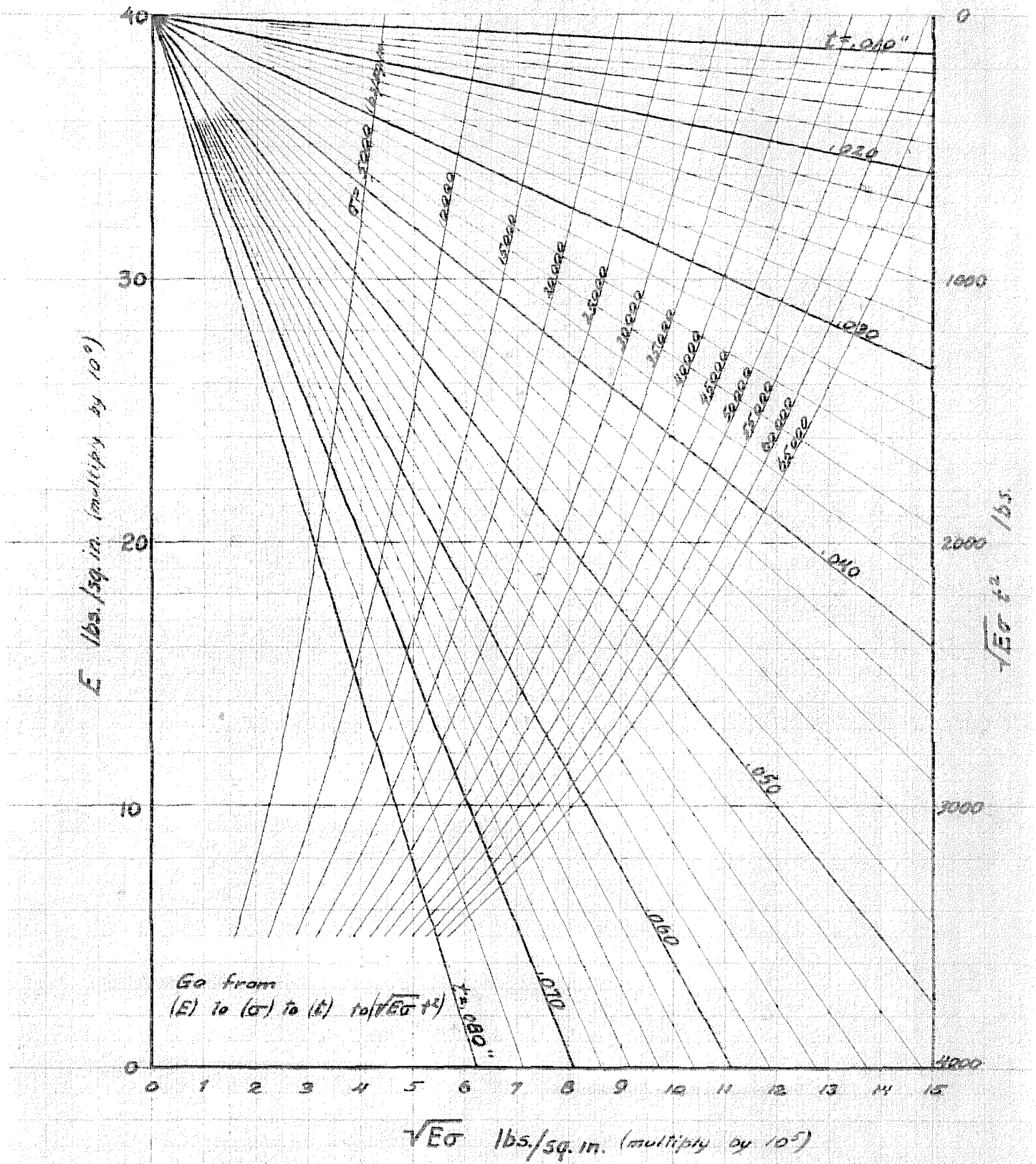

Fig. B-6

Curve for the Determination of $\sqrt{E\sigma}\, t^2$

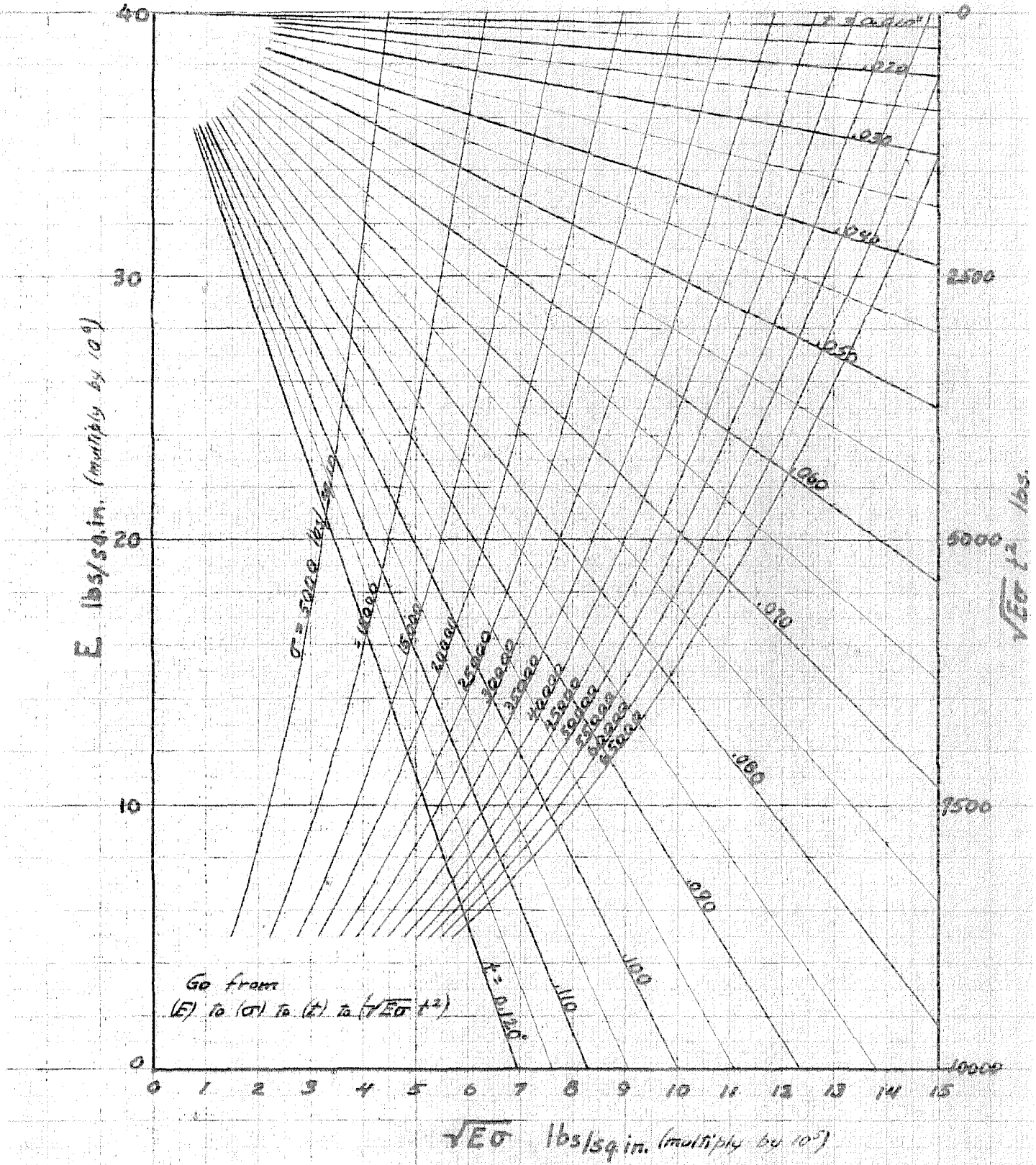

Fig. B-7

CURVE FOR THE DETERMINATION OF C

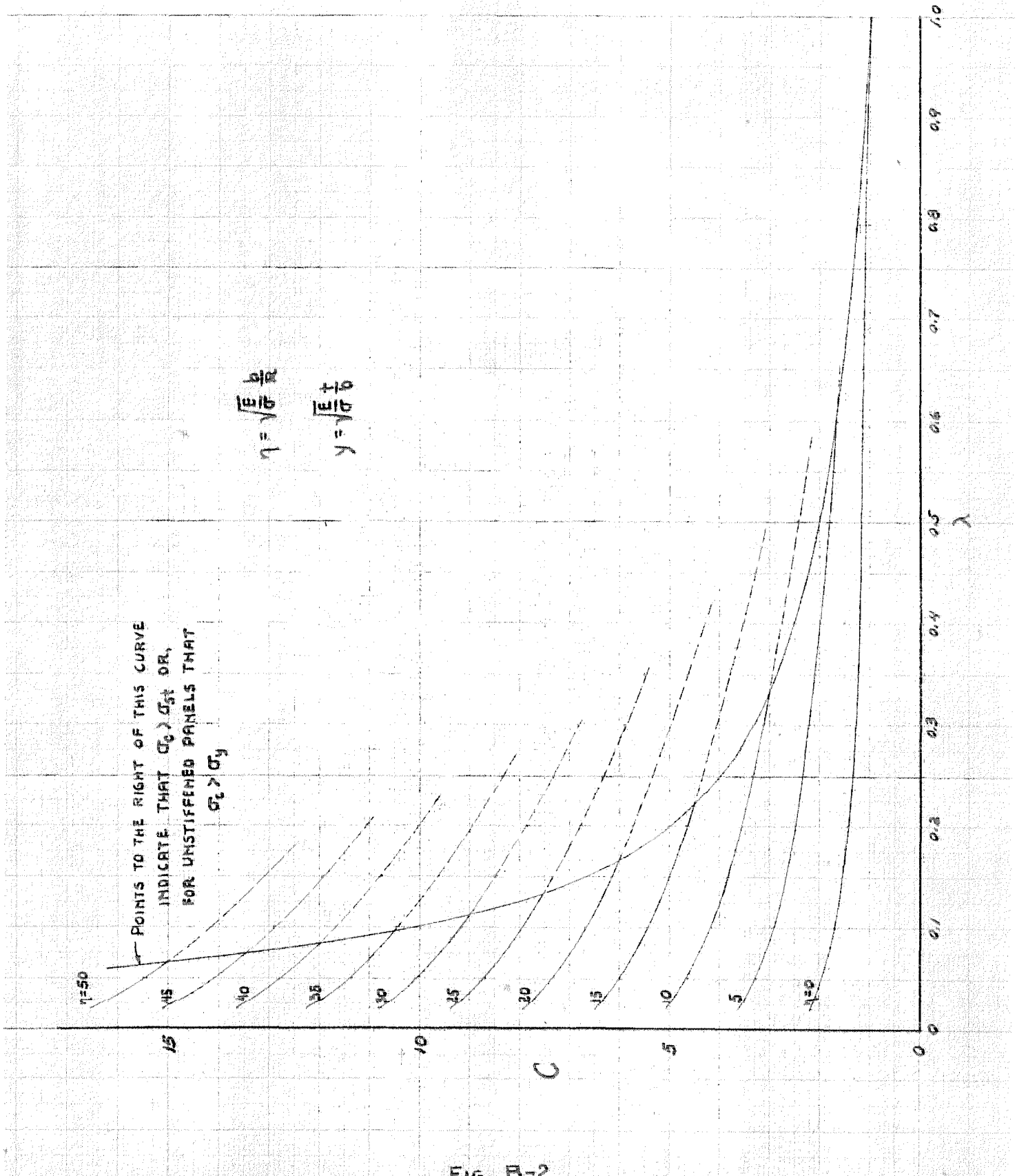

FIG. B-2

CURVE FOR THE DETERMINATION OF $\left(\frac{\rho}{\rho_o}\right)^2 = \frac{\sigma}{\sigma_o}$

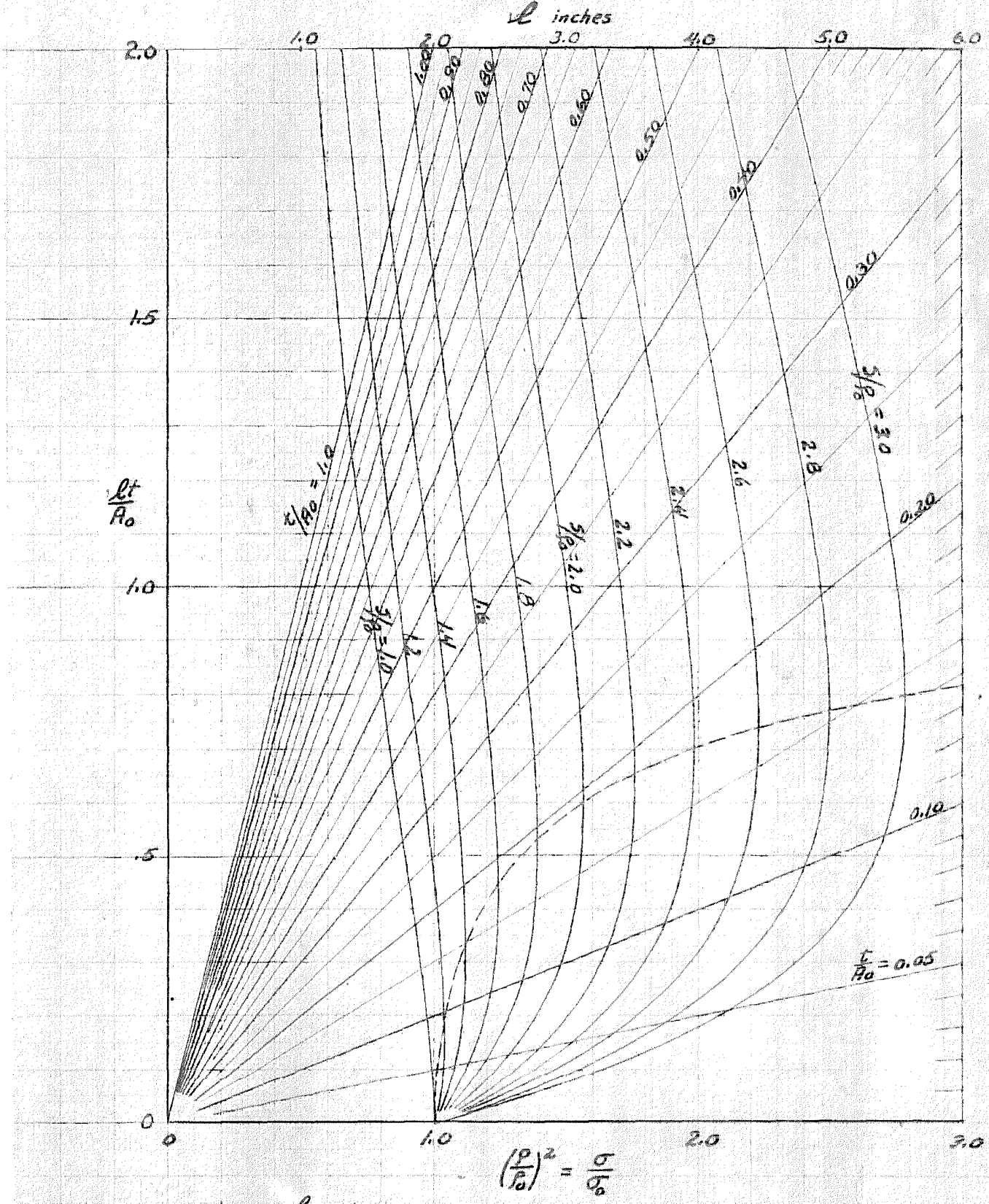

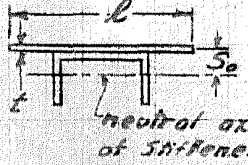

A_0 = Area of Stiffener

METHOD:

Go from $\frac{\ell}{f_0} - \frac{t}{f_0} - \frac{t}{f_0}\frac{s}{\rho_0} - f_0 - \left(\frac{\rho}{\rho_0}\right)^2$

or from $\frac{\ell t}{A_0} - f_0 - \frac{s}{\rho_0} - f_0 - \left(\frac{\rho}{\rho_0}\right)^2$

Fig. B-3